Calcium isotope cosmochemistry

Maria C. Valdes, Katherine R. Bermingham, Shichun Huang, Justin I. Simon

PII: S0009-2541(21)00339-9

DOI: https://doi.org/10.1016/j.chemgeo.2021.120396

Reference: CHEMGE 120396

To appear in: Chemical Geology

Received date: 18 June 2019

Revised date: 4 June 2021

Accepted date: 8 June 2021

Please cite this article as: M.C. Valdes, K.R. Bermingham, S. Huang, et al., Calcium isotope cosmochemistry, *Chemical Geology* (2021), https://doi.org/10.1016/j.chemgeo.2021.120396

This is a PDF file of an article that has undergone enhancements after acceptance, such as the addition of a cover page and metadata, and formatting for readability, but it is not yet the definitive version of record. This version will undergo additional copyediting, typesetting and review before it is published in its final form, but we are providing this version to give early visibility of the article. Please note that, during the production process, errors may be discovered which could affect the content, and all legal disclaimers that apply to the journal pertain.

© 2021 Published by Elsevier B.V.



Calcium Isotope Cosmochemistry

Maria C. Valdes^{a,b,c,*} mvaldes@fieldmuseum.org, Katherine R. Bermingham^{d,e}, Shichun Huang^f, Justin I. Simon^g

^aRobert A. Pritzker Center for Meteoritics and Polar Studies, Negaunee Integrative Research Center, The Field Museum of Natural History, Chicago, USA

^bDepartment of Geophysical Sciences, The University of Chicago, Chicago, IL, USA

^cDepartment of Earth Sciences, University of Cambridge, Cambridge, UK

^dDepartment of Earth and Planetary Science, Rutgers University, Liscataway, NJ, USA

^eDepartment of Geology, University of Maryland, College Park, ML USA

^fDepartment of Geoscience, University of Nevada, Las Vega, Las Vegas, USA

^gCenter for Isotope Cosmochemistry and Geochropology, Astromaterials Research and Exploration Science, NASA Johnson Space Center, Houston, USA.

for Chemical Geology special issue on Callium Isotopes: Past lessons and future directions

Abstract

The past decade has see: significant advancements in analytical capabilities and with it a marked increase in the use of Ca isotopes to advance our understanding of the Solar System's and Earth's evolution. Here, neass-dependent and non-mass-dependent Ca isotopic variations in bulk meteorites and chartity components are discussed. This contribution also examines how Ca isotopes record neb lar processes, including evaporation/condensation and mixing of chemically and isotopically distinct reservoirs in the protoplanetary disk. The applicability of non-mass-dependent Ca isotopic variations to tracing the nature and timing of stellar mass contributions to the parental molecular cloud is discussed. This includes the constraints Ca isotopic data provide on the nature of and the relationships between planetary building blocks. This contribution also explores the effects of parent body-based and terrestrial secondary processes, and variable sampling of isotopically heterogeneous Ca-rich components, on bulk meteorite compositions. Using the data reviewed here, this contribution attempts to reconcile the chemical and isotopic Ca data from bulk meteorites and meteorite components to address a major goal in planetary science, the development of a comprehensive model of the chemical and isotopic evolution of the Solar nebula into our planetary system.

^{*}Corresponding author.

Keywords

Calcium isotopes; cosmochemistry; Meteorites; CAIs

1. Introduction

Understanding how a habitable planet formed requires an understanding of how its host planetary system and star evolved. The study of major elements and their isotopes, such as Ca, provides key constrains on the chemical evolution of the Solar System. The generalities of the process are understood, but much of the detail is yet to be revealed.

The Solar System originated from a portion of a parent 1 molecular cloud which was composed of dust and gas that had accumulated from earlier generation stars. This includes dust that was added to the interstellar medium at least $\sim 3 \pm 2$ Ga pric to the start of the Solar System (Heck et al., 2020). The cause of the separation between the prote-nebula and the main molecular cloud mass is debated (for a review, see Montmerle et al. 2006). It may have been caused by shockwaves from a neighboring supernova (Cameron at d.) uran, 1977; Boss, 1995) or sufficient weakening of the magnetic field support following ambigular diffusion (Shu et al., 1987). This fragment formed a rotating disk (generally refer ec to as a protoplanetary disk) nested in the molecular cloud. At the center of the protoplane ary Lisk, the "proto-sun" began hydrogen fusion when sufficiently high temperature and pre-sure were reached. Subsequently, planets, their satellites grew out of the protoplanetary lisk via accretion, a process that describes the coalescence of um-sized solid particle; into cm-sized pebbles, km-sized planetesimals, and finally the planets (for reviews, see Jonainen and Lambrechts, 2017; Simon et al., 2018). Most of the material that did not accrete to the planets or their satellites remains in the Solar System as asteroids, where the majority of this mass is stored in the main asteroid belt (equivalent to ~4% of the Moon's mass) and lies between Mars and Jupiter. Some parent bodies in the asteroid belt are sampled by Earth in the form of meteorites. As remnants of the protoplanetary disk, meteorites can be used to constrain the chemical (e.g., elemental abundances) and isotopic building blocks of the Solar System and planets.

Meteorites are Chadly classified into two groups: chondrites, which originate from unmelted (undifferentiated) parent bodies, and achondrites, which originate from melted (differentiated) parent bodies. Both groups provide important chemical and isotopic constraints on Solar System evolution. For example, through the comparison of element abundances in unmelted meteorites to the Sun's photosphere, it was concluded that CI chondrites provide the closest chemical match to the non-volatile¹ composition of the Solar nebula (Anders, 1971). Element abundances in meteorites have since been used to infer element fractionation due to nebular processing and parent-body igneous processes (e.g., Nittler et al., 2004). In combination

_

¹ Refractory elements have 50% condensation temperatures (T_c) above 1335 K, moderately volatiles between 1335 and 665 K, volatile elements below 665 K, and highly volatile elements below 371 K. Condensation temperatures refers to the equilibrium condensation appearance temperature of an element into a compound (solid phase) from a Solar composition gas at 10⁻⁴ bar total pressure (Lodders, 2003).

with planetary observations, these and other chemical data obtained from meteorites indicate a relatively volatile depleted inner Solar System *vs.* a volatile enriched outer Solar System. Here, the inner and outer Solar System refers to inboard or outboard of Jupiter (following Warren, 2011).

Chondrites preserve discrete meteorite components that formed in the disk prior to the accretion of the parent body. The meteorite components were likely sampled by achondrite parent bodies to varying degrees; however, differentiation mixed these components into the bulk composition of the body such that they are no longer visible. There are several types of refractory inclusions, chondrules, dark fragments, and dark inclusions found in chondrites. Here, these materials are collectively referred to as "chondrite components" and the constraints their Ca isotopic compositions provide on early Solar System evolution are discussed in Section 3. Calcium-aluminum-rich inclusions (CAIs) are one type of refractory factusion which are among the first aggregates that formed from disk material. These refractor, inclusions have an average condensation age 4567.30 ± 0.16 Ga (Connelly et al., 2012) and in most cosmochemical studies this age defines "time zero" (t₀) and the start of the Solar System. The primary mineralogy of these inclusions is enriched in refractory elements (e., C1, Al, and Ti) as oxides or silicates, which are among the first phases predicted to condense from a cooling gas of Solar composition (Grossman, 1972; Yoneda and Grossman, 1995; I'e'ac v and Wood, 1998). As indicated by their complex mineralogy, CAIs experienced multiple heating and cooling events prior to incorporation into larger bodies (e.g., Petz ev and Jacobsen, 2009). The coexistence of refractory inclusions and volatile elements (e.g., C, N, \Im) in some carbonaceous chondrites indicates large temperature gradients in the disk and mixing between different regions during the formation of some parent bodies.

Despite the different envir morents and thermal/chemical processing that occurred in the disk, a record of presolar dust is intained in meteorites (e.g., Lewis et al. 1987; Zinner et al. 1987; Dauphas et al. 2010; Me. dybaev et al., 2002; Simon et al., 2019). Although only unmelted meteorites preserve these oraine such that they can be isolated by chemical treatment, presolar dust was inherited by both rielted and unmelted meteorites (Zinner, 2014). Presolar grains, a type of presolar dust, for red in stellar outflows or ejecta and remained intact throughout their journey into the Solar System where they were preserved in meteorites (Lodders and Amari 2005). Because presolar grains contain isotopes in relative abundances reflective of the stellar environment in which they formed, these grains have very different (vary on the ‰- to %-scale) compositions compared to material that formed from the protoplanetary disk (e.g., Burbidge et al., 1957; Cameron, 1957; Clayton et al., 1973; Lewis et al., 1987; Bernatowitz et al., 1987; Zinner et al., 1987; Amari et al., 1990; Zinner, 2014). It is generally considered that presolar grains were heterogeneously distributed in the protoplanetary disk, where some grains may have been introduced to the Solar nebula after its initial accretion. The heterogeneous distribution of presolar material is indicated by the existence of variable non-mass-dependent isotopic compositions (so-called nucleosynthetic isotopic variations) in bulk meteorites and their components (see review by Qin and Carlson, 2016). By studying non-mass-dependent isotopic

compositions in meteorites and their components, the stellar events that contributed material to the Solar System and their distribution in the protoplanetary disk can be identified.

This review synthesizes Ca isotopic variations in bulk meteorites² and their components with the constraints these data provide on the early stages of Solar System evolution. The focus is on how mass-dependent and non-mass-dependent Ca isotope effects provide information about the compositions of cosmochemical building blocks, thermal processing in the disk, and parent body alteration. It concludes with a summary of outstanding questions in cosmochemistry and the future avenues of research Ca isotopes present.

1.1. The role of Ca in cosmochemistry

Calcium is one of the most refractory elements in the Colar System ($T_c = 1659 \text{ K}$; Lodders, 2020). Consequently, some Ca condensed into CAIs and other early formed meteorite components, thereby preserving chemical and isotopic information count the early disk. As Ca is a major component in asteroids (e.g., \sim 1-8 wt% in HEDs, Mutlefehldt, 2014) and terrestrial planets (2.52 wt% in bulk silicate Earth; McDonough and Sun, 1995), it can also be used to investigate parent body compositions, differentiation (Huang et al., 2010), and parent body alteration (Zolensky and McSween, 1988).

The utility of the Ca isotope system stems in the high number of stable Ca isotopes and the mass range they cover, the existence of a short-lived radioactive Ca isotope, and the diversity of nucleosynthetic pathways that produce Ca isotopes. Calcium comprises twenty-four isotopes, six of which (40³, 42, 43, 44, 46, and 48⁴) are considered to be stable isotopes (Amos et al, 2011). The 20% range between the hehtest and heaviest stable Ca isotopes is more than any element except for H and He (Clay or 1, 2004), which makes Ca isotopes a sensitive tool for recording mass-dependent isotopic fractionation. Cosmochemical Ca isotope studies exploit these features to track processes that generate Ca mass-dependent isotope fractionation, including nebular condensation and evaporation, parent body differentiation, and aqueous alteration.

Non-mass-depandant Ca isotopic compositions preserve information about the stellar sources that contributed paterial Solar nebula and how these were distributed in the disk (e.g., Dauphas et al., 2014a). The dominant nucleosynthetic pathways for Ca are listed in **Table 1** and for detailed review of Ca isotope nucleosynthetic pathways and stellar sources see Burbidge et al. (1957), Meyer (1996), and Wanajo et al. (2013). Also of cosmochemical relevance is the short-lived radioactive system 41 Ca $^{-41}$ K (41 Ca 41 Ca 41 Ca in early Solar System came from correlating 40 Ca. The first definitive evidence for live 41 Ca in early Solar System came from correlating 41 K/ 39 K ratios with Ca/K in Efremovka (CV3) CAIs (Srinivasan et al. 1994, 1996), and subsequent studies of hibonites from Murchison (CM2) and Allende (CV3) (Sahijpal et al.,

² Bulk meteorite refers to a homogenized sample of the entire meteorite, as opposed to a sample of distinct meteorite components.

 $^{^{3}}$ 40 Ca abundances can be affected by the β-decay of 40 K (40 K $t_{1/2}$ = 1.25 Ga).

 $^{^{4}}$ 48 Ca is radioactive with a $t_{1/2}$ of 4.3 x 10^{19} years; however, its long half-life permits it to be considered a stable isotope.

1998, 2000). Newer data on the same and additional CAIs (from NWA 3118 and Vigarano, both CV3) indicate that the early Solar System ⁴¹Ca/⁴⁰Ca was lower than indicated in earlier works (Liu et al., 2012; Liu, 2017). Cosmic ray exposure ages can be calculated for meteorites and lunar soils using this short-lived radioactive system (Bogard et al., 1995; Nishiizumi et al., 1997).

2. Background

2.1. Calcium isotope basics and nomenclature

The Ca isotope ratio determinations of Russell et al. (1978) provide the basis for current measurements. Established on sample measurements where radiogenic 40 Ca/ 44 Ca excesses are negligible, these values are used to represent the normal terrestric. composition at about 0.01% precision. Modern 40 Ca/ 44 Ca and 43 Ca/ 44 Ca measurements of in fix achondrites and oceanic basalts by Simon et al. (2009) were used to reevaluate the initial terrestrial Ca isotopic composition. Assuming the normal 42 Ca/ 44 Ca = 0.31221 of Rus sell et al. (1978), the weighted means of these measurements yield 40 Ca/ 44 Ca = 47.1480 ± 20 0004 (2 20) and 43 Ca/ 44 Ca = 0.064868 ± 0.000001 (2 20) that are consistent with the previous determinations by Russell et al. (1978) showing that at the bulk rock scale many planetary materials exhibit a homogenous Ca isotopic composition. It should be noted that Simon et al. (209) report a resolvable (+0.05 to +0.1%) 40 Ca/ 44 Ca excess for the commonly used carbonate standard SRM915a5. More recently, and also at higher precision, 43 Ca/ 44 Ca, 46 Ca/ 44 Ca and 48 Ca/ 44 Ca measurements show that some bulk meteorites exhibit resolvable 48 Ca/ 44 Ca anona lies (Dauphas et al., 2014a, Schiller et al. 2015, as discussed in more detail below).

For radiogenic enrichment a κ nucleosynthetic heterogeneity studies, non-mass-dependent Ca isotopic variations are commonly reported as $\epsilon^x \text{Ca}/^{44}\text{Ca}$ (equal to 10^4 ((\frac{4x}{Ca}/^{44}\text{Ca})_{sample(N)}/(\frac{4x}{Ca}/^{44}\text{Ca})_{s. ndard(N)} - 1))), where x is 40, 42, 43, 46, 48, and subscript N refers to internal normalization in trinsic to the sample. The normalization value, however, is dependent on the choice of mass fractionation law, and the same law is not necessarily appropriate for both instrumental and intrinsic fractionation (see Zhang et al., 2014).

In the early literature, stable Ca isotope studies used δ^{40} Ca/ 44 Ca notation (equal to 10^3 ((40 Ca/ 44 Ca)_{sample}/(40 Ca/ 44 Ca)_{standard} – 1)) as a measure of the natural isotopic variations, including both mass-dependent and non-mass-dependent, intrinsic to the sample. This notation has the somewhat confusing consequence where natural mass-dependent heavy isotope enrichments lead to negative delta values (Russell et al. 1978). Skulan et al. (1997) used the Russell et al. (1978) ratios as references for assessing natural mass-dependent isotopic variation, and introduced the δ^{44} Ca/ 40 Ca designation (equal to 10^3 ((44 Ca/ 40 Ca)_{sample}/(44 Ca/ 40 Ca)_{standard} – 1)), which is more consistent with the notation used for other stable isotope systems, where the heavier isotope is in the numerator such that the high values for both the isotope ratio and delta value represent

⁵ See similar reports discussed in the high-temperature geochemistry contribution (Antonelli and Simon, 2020) to this special issue.

relative enrichment of heavy isotopes. This δ-notation is adopted by most recent stable Ca isotope studies; however, we note that this tradition is not strictly followed in literature as most non-mass-dependent Ca isotopic data for meteorite components are reported using δ-notation. It is important to note that the most abundant isotope, 40 Ca, is also one of the radioactive decay products of 40 K (half-life of ~1.25 Ga). δ^{44} Ca/ 40 Ca therefore includes potential radiogenic ingrowth of 40 Ca in the samples. This complication can be avoided by either measuring δ^{44} Ca/ 42 Ca and then converting to δ^{44} Ca/ 40 Ca by multiplying by approximately 2^6 (e.g., Huang et al., 2012; Fantle and Tipper, 2014; Valdes et al., 2014; 2019; Zhang et al., 2014; He et al., 2017; Amsellem et al., 2017, 2019), or by measuring 44 Ca/ 40 Ca directly and then correcting for radiogenic 40 Ca ingrowth using additional (unspiked) measurements when necessary.

In this review, when the terms "anomalous" or "variable are used, we refer to mass-dependent isotopic compositions which, with consideration of their internal and external errors, depart from what is expected by mass-dependent fractionation and fall outside the range of values estimated for bulk Earth or the terrestrial standard referenced in the study. Regarding non-mass-dependent isotopic compositions, the terms refer to Ca isotopic compositions that fall outside the composition of a terrestrial standard. As analytical precision improves, subtle radiogenic enrichment effects in samples, and the propagation of poorly recognized isotopic artifacts in standard materials and those potentially produced during instrumental mass bias correction, need to be considered as possible explanations for observed Ca isotopic variation.

There are currently more than four different reference values commonly used in the modern literature for Ca isotope measurements (including CaF₂, Bulk Silicate Earth "BSE", modern seawater, and artificial calcium carbonates SRM915a and SRM915b). Although the SRM915a standard is no longer commonally available, it is presently still used in the majority of cosmochemical studies. Those studies that used BSE as a reference value have estimated its Ca isotopic composition relative to JRM915a (δ^{44} Ca/ 40 Ca_{BSE-SRM915a}) in a number of ways. For example, Huang et al. (2010) no deled δ^{44} Ca/ 40 Ca_{BSE-SRM915a} from the Ca isotopic compositions of the principal Ca-bearing minerals in mantle peridotites. More recently, Kang et al. (2017) estimated δ^{44} Ca/ 40 Ca_{BSI-SR-M15a} through the measurement of spinel and garnet lherzolites. The different approaches yield nearly identical values (+1.05 ± 0.04 vs. +0.95 ± 0.05, respectively; see Antonelli and Simon (2020) and discussion therein).

Here, +0.95 is adopted as the Ca isotopic composition of BSE relative to SRM915a because this estimate is based on a larger sample set. In order to facilitate inter-study comparison, all data discussed have also been converted to both SRM915a and BSE scales $(^{44}\text{Ca}/^{40}\text{Ca}_{BSE} = \delta^{44}\text{Ca}/^{40}\text{Ca}_{SRM915a} - 0.95)$ in **Supplementary Table 1.** For the remainder of this review, SRM915a composition is referred to as "Earth" and data discuss as referenced to SRM915a. For original data and conversion information, see **Supplementary Table 1**. Positive $\delta^{44}\text{Ca}/^{40}\text{Ca}$ indicate heavy isotopic compositions and negative $\delta^{44}\text{Ca}/^{40}\text{Ca}$ indicate light isotopic compositions. Non-mass-dependent data are referenced to the standard reported in the relevant

 $^{^{6}}$ 2.05 for the canonical exponential mass law, 1.93 for the Rayleigh law which may be associated with kinetic isotopic fractionation, or 2.10 for the equilibrium mass law.

reference, where the mass fractionation law and reference ratios reported are summarized in **Supplementary Table 1**. While it is possible that differences in reporting non-mass-dependent data may cause issues when comparing datasets, since non-mass-dependent data are always reported relative to a terrestrial standard, the subtle difference in the calculated mass fractionation corrected ε -values introduced by those different approaches is comparable or smaller than the reported analytical uncertainty.

2.2. Theoretical mass-dependent fractionation models

Theoretical and experimental studies provide a basis for understanding the stable isotopic composition of planetary materials, in particular isotope effects related to evaporation at low pressures (Esat et al., 1986; Davis et al., 1990; Grossman et al., 2000; Humayun and Cassen, 2000; Nagahara and Ozawa, 2000; Richter et al., 2002; Young a. l., 2002; Zhang et al., 2014; Davis et al., 2015). Such studies imply that evaporative residue, must have been heated at low pressures to produce appreciable mass-dependent isotopic fractic nation (Esat et al., 1986; Davis et al., 1990; Young et al., 1998; Richter et al., 2002; Yam, da et al., 2006; Richter et al., 2007; Shahar and Young, 2007; Knight et al., 2009; Zhang et al., 2014). As such, the heavy Mg and Si isotope enrichments of many CAIs require that they experienced evaporation at low pressures (<10⁻⁴ bar), conditions that are thought to be typi 2.1 ear the proto-Sun. In contrast, the normal Mg and Si isotopic compositions reported in so, re parts of CAIs (Bullock et al., 2013; Simon et al., 2005) and for chondrules (Galy et al. 2010; Cuzzi and Alexander, 2006; Alexander et al., 2008) imply that these materials formed nom high local partial pressures and/or dust-rich regions of the Solar nebula distinct from the hot inner Solar nebula. Thus, the degree of enrichment of heavier Mg and Si isc to be in disk materials provides evidence of heating and a record of the pressure, possibly due to the local concentration of solids under which they formed (Cuzzi and Alexander, 2006).

To test models for mas, tractionation related to evaporation, it is useful to compare the refractory Ca isotopic signature in early formed solids to that of moderately volatile element isotopic signatures, such as Mg. Because of its highly refractory nature, Ca isotopic signatures record early mass-depend int isotope fractionation. In contrast, Mg isotopic records preserved in individual CAIs may be dominated by the last isotopic exchange event, overprinting the record of the earliest stages of nebular evolution.

Comparison of Ca and Mg isotopic data for CAIs (e.g., Niederer and Papanastassiou, 1984; Simon et al., 2017) and numerical models demonstrates the apparent inconsistency between Ca and Mg isotope effects (**Fig. 1**). There remains a limited number of samples in which Ca isotopes have been measured along with Mg, and many of these are FUN (Fractionated with Unknown Nuclear effect) inclusions. Because of the relatively large uncertainty (± 3 %) in δ^{44} Ca/ 40 Ca ratios reported by early Ca isotope studies, more high precision measurements are needed to fully interpret the interrelationships between Ca and Mg effects in chondrite components. Though the analytical precision of Ca isotopes has significantly improved, it is worth noting that current mass spectrometry methods may require further refinement. This is

especially true where large naturally occurring isotope fractionation that occurred during CAI formation may not follow an exponential fractionation law (e.g., Lee et al., 1979; Ireland et al., 1992). As such, current instrumental mass bias corrections could lead to apparent non-massdependent isotope anomalies (see Huang et al., 2012; Zhang et al., 2014). Nevertheless, published results support the hypothesis that enrichment of heavy Ca isotopes arose from extensive evaporation of CAIs (Zhang et al., 2014) followed by later addition of less fractionated Mg (see Fig. 1). This could be analogous to the "flash heating" hypothesis (Wark and Boynton, 2001) used to explain the formation of spinel-hibonite Wark-Lovering rim layers surrounding many CAIs. More generally, it is critically important to understand the range of temperature conditions as well as the effects of open system isotopic exchange, because both have implications for the nebular settings in which chondrite componer's formed and evolved. Such insights may help reconcile some of the differences reported for Al-Mg chronologies between different nebular materials and studies (e.g., Simon and Young 2011; MacPherson et al., 2012), and/or the observed abundances of various short-lived rad anu lides. For example, this could help explain why the abundances of both 41Ca and 5Al tend to be correlated, but are unexpectedly absent in some CAIs (Goswami, 2001; Sinivasan et al., 1996; Liu, 2017). Integrating these isotopic signatures in nebular materials is essential to understand the connections between distinct nebular environment; in pace and time.

Kinetic isotopic fractionation effects during condensation and evaporation have been modeled (e.g., Humayun and Cassen, 2000; Simon and DePaolo, 2010; Simon et al., 2017). Simon et al. (2017) compiled studies with notifielement isotopic measurements of CAIs to test the latest condensation model. These comparisons help to evaluate the isotopic consequences of condensation from a nebular gas considering the kinetics of condensation, the degree of undercooling, and potential reservou effects. While it is possible to directly measure fractionation factors for evaporation (α_{evap}) in the laboratory, this is not the case for condensation fractionation factors (α_{cond}). In fead, a condensation model is needed to indirectly obtain α_{cond} . Invoking the law of mass region, Simon et al. (2017) showed that: $\alpha_{\text{eq}} = \frac{\alpha_{\text{cond}}}{\alpha_{\text{evap}}}$. Equilibrium fractionation factors can be calculated or measured experimentally, allowing one to solve for α_{cond} (Simon et al., 2017)

Kinetic isotopic fractionation during condensation depends upon the relative roles of collisional frequency (between gas species and the grain surface), compared to the ability of a gas species to incorporate into the condensed phase (Simon and DePaolo, 2010). Partition of the lighter isotopes into the condensates is favored when collisional frequency is the dominant controlling effect. In the nebula, the magnitude of fractionation is mainly controlled by both the speciation transformed from vapor to solid or vice versa, and the degree of evaporation or condensation. Zhang et al. (2014) showed experimentally that when an element, Ti in this case, has more than one significant evaporating species, this can be important (see Simon et al., 2017 for a worked example that accounts for both TiO and TiO₂ in the vapor phase). For Ca, one can assume a simpler scenario in which α_{eq} , for any given solid-vapor reaction, only has Ca in the

vapor phase. This can be justified because at realistic nebular conditions Ca >> CaO in the vapor phase (Zhang et al., 2014).

Ultimately, the relative importance of equilibrium versus kinetic isotope effects in isotope fractionation depends on the degree of exchange "overstepping" as measured by the saturation index $S_i = P_i/P_{i,eq}$, with $S_i > 1$ implying condensation. S_i can be equated with a temperature difference (e.g., undercooling) from the equilibrium condensation temperature using the Van't Hoff equation and the enthalpy for the condensation reaction (Simon and DePaolo, 2010).

This model shows that for fractionation during condensation (Simon and DePaolo, 2010; Simon et al., 2017):

$$\alpha_{\mathrm{cond}} = \frac{\alpha_{\mathrm{eq}} \alpha_{\mathrm{kin}} S_{\mathrm{i}}}{\alpha_{\mathrm{eq}} (S_{\mathrm{i}} - 1) + \alpha_{\mathrm{kin}}} \quad \text{where} \quad \alpha_{\mathrm{kin}} = \alpha_{\mathrm{evap}} \alpha_{\mathrm{eq}} \sqrt{\frac{m_{i}}{m'_{i}}}$$

with m_i and m_i being the masses of the lighter and heavier isotopes of the species of interest, respectively. A preliminary comparison of coordinated multipale nent measurements can be made to the condensation model (**Fig. 2**). Other than showing that heterogeneity exists, the early TIMS data (open symbols) are insufficiently precise to constrain the model. The steadily growing data available (e.g., Huang et al., 2012, Simon et al., 2017, Bermingham et al., 2018), however, allows us to quantify the undercooling associated with condensation. Moreover, we see clear evidence that various CAI types formed from M3 isotopic reservoirs that are distinct from that which is "normal" to planetary bodies (see also Huang et al., 2012 and Bermingham et al., 2018, summarized in **Section 3.2.6**, for further information on this interpretation). We expect clarity on these promising findings when more precise measurements are made on a representative suite of CAIs.

3. Calcium isotope constraints or the origin of chondrite components

Early meteorite studies exploited the naturally high Ca concentrations in meteorite components to collect coupled mass-dependent and non-mass-dependent Ca isotopic data (e.g., Lee et al., 1978,1979; Niederar and Papanastassiou, 1984; Ireland, 1990; Ireland et al., 1991, 1992). The elemental and iso opic compositions of chondrite components provided some of the first sample-based constraints on the thermal and chemical characteristics of the disk. Here, studies reporting Ca isotope ratios in chondrite components are reviewed and a synthesis of these data is presented. Although the emphasis of this review is on Ca isotopes, the significance of chondrite component Ca isotopic data in deciphering Solar System evolution is bolstered when interpreting the data in the context of Ti, Mg, and O isotopic data and rare earth element (REE) abundance data.

3.1. Refractory inclusions

Refractory inclusions are small (µm to cm) objects that are dominated by refractory Al, Ca, Ti, Mg, and Si oxides. Refractory inclusions in CM chondrites have higher abundances of hibonite and spinel compared to Ca-Al-rich silicates in CV chondrites (MacPherson et al., 1983). Rare earth elements are trace in abundance in refractory inclusions. Their relative fractionation

patterns are highly variable as a result of the inclusions undergoing complex thermal processing in the disk prior to accretion to a parent body (e.g., Boynton, 1975; Davis and Grossman, 1979; Ireland, 1988). Based on mineralogy and elemental composition, refractory inclusions can be grouped into the following types hibonite-bearing refractory inclusions, Ca-Al-rich silicate CAIs (Type $1 - VI^7$; Martin and Mason, 1974; Mason and Taylor, 1982), and ameboid olivine aggregates (AOAs).

3.1.1. Hibonite-bearing refractory inclusions

Hibonite-bearing refractory inclusions are smaller (µm-scale) than Ca-Al-rich silicate CAIs and AOAs (mm- to cm-scale); however, their isotopic variations can be an order of magnitude or more anomalous (Fig. 3). Hibonite-bearing refractor inclusions are predominantly found in CM2, but some have been found in CV3, CO3, CR, and H2 chondrites. These refractory inclusions preserve early disk chemistry because hibonite is predicted to be one of the first major element-bearing phases (after corundum) to condense from the Solar gas (Grossman, 1972; Davis et al., 1982) or it is the distillate of Solar gas evaporation (Ireland et al., 1992). There are at least five principal types of hibonite-bearing inclusions, which are distinguished on the basis of petrography and morphology. This includes Blue Argregates (BAGs), hibonite-bearing spherules, HAL-type inclusions (HAL-type), PLAty hibonite Crystal fragments (PLACs), and Spinel-HIBonite spherules (SHIBs) (but see Yöop et al., 2016a for a description of some hibonite-rich objects in Murchison which to not clearly fall into these morphological categories).

3.1.1.1. BAGs

Blue AGgregates are rare hisomorphic in control refractory inclusions found in CM chondrites. They are pleochroic blue (as observed using an optical microscope) bladed hibonite crystal aggregates and comprise crystal plates and fragments. Blue AGgregates typically have similar TiO₂ (5.1 to 6.5 %), low trace element abundances with large relative depletions in ultrarefractory elements (Group 'I-like patterns), and an absence of spinel (Ireland, 1988; 1990).

Only one BAG (13-23) has been documented for Ca isotopic compositions (Ireland, 1990). This inclusion does not display Ca or Ti isotope mass-dependent fractionation, but it is depleted in ϵ^{48} Ca/ 44 Ca (-133 \pm 47) and ϵ^{50} Ti/ 48 Ti (-227 \pm 31). Other BAGs that have been analyzed have similar depletions in 50 Ti; however, BAG 10-31 has a near-normal 50 Ti composition (Ireland, 1990). Inclusion 13-23 and other BAGs possess heavy mass-dependent Mg isotopic compositions (Δ^{25} Mg 8). Generally, mass-independent δ^{26} Mg 9 isotopic compositions have been linked to in-situ decay of short-lived radioactive isotope 26 Al ($t_{1/2} \sim 0.7$ Ma). Typically, BAGs have unresolved δ^{26} Mg compositions (e.g., BAG 13-23) from the standard, or are depleted

⁷ Group IV CAIs are mainly composed of chondrules.

⁸ Δ^{25} Mg refers to mass-dependent Mg isotopic compositions, where positive Δ^{25} Mg is defined as an enrichment in the heavy isotopes relative to terrestrial Mg (Ireland, 1988).

 $^{^9}$ δ^{26} Mg refers to non-mass-dependent Mg isotopic composition from which the radiogenic component from live 26 Al can be determined (Ireland, 1988) where canonical 26 Al/ 27 Al $_0$ is $\sim 5.3 \times 10^{-5}$ (MacPherson et al., 1995; Jacobsen et al., 2008; Larsen et al., 2011).

in ²⁶Mg which could suggest some BAGs did not contain live ²⁶Al (Ireland, 1988; 1990; Liu et al., 2009). The combined isotope and trace element data are consistent with BAGs being condensates from a gas from which lower temperature components have been removed (Ireland, 1990). Given the rarity of BAGs and the absence of multi-element and isotopic datasets, however, the origin of these inclusions remains poorly constrained.

3.1.1.2. Hibonite-bearing spherules

Hibonite-bearing spherules comprise a rare subset of refractory inclusions identified in CM2, CO3, and CH3 meteorites (Ireland et al., 1991; Russell et al., 1998). These spherules contain hibonite and silicate glass, or are glass-free but contain hibonite and pyroxene. From Ireland et al. (1991) and Russell et al. (1998), hibonite-bearing spacrules display a range of REE abundance patterns, including Group II patterns. Characteristically, hibonite-bearing spherules record large, coupled excesses in ϵ^{48} Ca/ 44 Ca (up to +400) and 50 Ci/ 48 Ti (up to +200) in both glass and hibonite, where each phase is similarly enriched. There is an absence of Ca and Ti mass-dependent isotope fractionation, except hibonite in the spherule (MUR7-228) is slightly light (δ^{44} Ca/ 40 Ca -11 ± 3) (Ireland et al., 1991). Maga siu n isotopes can be mass-fractionated (heavy, in both glass and hibonite) (Ireland et al., 19°1). Generally, hibonite-bearing spherules are depleted δ^{26} Mg which infers an absence of 26 A', however, hibonite in MUR7-228 recorded evidence of 26 Al as an excess of δ^{26} Mg (Jraland et al., 1991). Because of the rarity of these inclusions, their petrogenesis remains un (ear, however, they may have formed via melting of various precursors under disequilibrium conditions and rapid cooling after hibonite crystallization (Ireland et al., 1991). The large excesses in ⁴⁸Ca and ⁵⁰Ti suggests they formed early in the disk, prior to incorporatio 1/st ²⁶Al.

3.1.1.3. HAL-type refractory in usions

Hibonite-bearing refractory inclusions are compositionally unusual hibonite-bearing inclusions. They include HAL (Libonite ALlende, from Allende), DH-H1 (from Dhajala, H3), 7-404 and 7-971 (from Mu. chis on), and Isna SP16 (from Isna, CO3.7). HAL-type inclusions have been studied extensively, where thus far HAL is the largest hibonite-bearing inclusion and is a FUN inclusion based on its highly anomalous O, Mg, Ca, and Ti isotopic compositions (e.g., Allen et al., 1979, 1980; Lee et al., 1979, 1980; Davis et al., 1982; Bischoff and Keil 1984; Hinton and Bischoff 1984; Fahey et al., 1987b; Hinton et al., 1988; Ireland et al., 1992; Russell et al., 1998; Sahijpal et al., 2000).

HAL-type inclusions display light (LREE) or heavy (HREE) REE enrichments, strong depletions in Ce and V or Yb, and they generally have low Mg and Ti concentrations compared to other hibonites (Fahey et al., 1987a; Hinton et al., 1988; Ireland et al., 1992; Russell et al., 1998). Samples HAL, DH-H1, 7-404, and 7-971 possess homogeneous non-mass-dependent depletions in ϵ^{48} Ca/ 44 Ca (~ -500) (except Isna SP16 which shows no variations in 48 Ca) and can be anomalous in ϵ^{50} Ti/ 49 Ti -40 (7-971) and +150 (HAL) (Ireland et al., 1992; Russell et al., 1998). HAL-type inclusions show non-correlated enrichments in heavy Ca (up to δ^{44} Ca/ 40 Ca

+53) and Ti isotopes¹⁰ (up to F_{Ti} +19; Ireland et al., 1992; Russell et al., 1998). Mass-dependent Ti isotope fractionation is inversely correlated with Ti concentrations (Ireland et al., 1992). HAL-type inclusions tend to display low inferred initial ²⁶Al/²⁷Al; however, Isna SP16 records a high initial ²⁶Al/²⁷Al (Lee et al., 1979; Fahey et al., 1987a; Ireland and Compston, 1987; Russell et al., 1998). Samples HAL, DH-H1, 7-404, and 7-971 are enriched in ¹⁶O relative to the terrestrial mean, and heterogeneous mass-dependent fractionation towards heavy O compositions (Lee et al., 1980; Ireland et al., 1992).

The origin of HAL and HAL-type inclusions is debated. Models suggest they are distillation residues (Lee et al., 1980; Ireland et al., 1992), or aggregates of condensate grains from a reservoir characterized by F and UN isotope signatures (Allen et al., 1980; Davis et al., 1982). Russell et al. (1998) concluded that the range in chemical and isotopic compositions of HAL-type inclusions suggests they formed by distillation of isotopic ally distinct mixtures of less refractory material. Regardless of the true formation process the variety in composition displayed by these inclusions in different meteorites (CV3, CM2, CO3, and H3) indicates that HAL-type hibonites are samples from different compositional regions of the disk at different times (following Russell et al., 1998).

3.1.1.4. PLACs and PLAC-like CAIs

PLAty-Crystals (PLACs) are one of two predominant hibonite crystal morphologies found in CM chondrites (Ireland, 1988). The other type of morphology is hibonite intergrown with Al-Mg spinel (Spinel-HIBonite spherules, SHIBs) which are discussed in the following section. PLAC hibonites are colorless (as observed with an optical microscope), small (≤150 µm) broken crystal fragments which are likely from larger inclusions and possess a restricted <2.7 % TiO₂ composition (Ireland, 1988; Loop et al., 2016a).

PLACs and hibonite-rich CAIs ("PLAC-like CAIs") are primarily found in CM chondrites and have been suched in detail. They record distinct chemical and isotopic compositions compared to other refractory inclusions (e.g., Ireland, 1988; 1990; Ireland et al., 1988; Lui et al., 2009; Kröp et al., 2016a; Kröp et al., 2018a,b). PLACs tend to be depleted in relatively volatile element's and display a decrease in HREE (e.g., Ireland et al., 1988; Ireland 1990). A characteristic isotopic feature of PLACs is that they possess the most isotopically anomalous (for Solar System-derived materials) non-mass-dependent ⁴⁸Ca compositions (ϵ^{48} Ca/⁴⁴Ca = -600 to +800) and ⁵⁰Ti compositions (ϵ^{50} Ti/⁴⁸Ti = -700 to -170; note PLAC 13-13 has anomalously high ϵ^{48} Ca/⁴⁴Ca = 1040 and ϵ^{50} Ti/⁴⁸Ti = 2730; Ireland, 1990; Kröp et al., 2016a). Most PLACs have the same mass-dependent Ca and Ti isotopic composition as the terrestrial standard (e.g., Ireland, 1990; Kröp et al., 2016a). As mass-dependent Ca and Ti isotope effects are small, non-mass-dependent Ca or Ti isotopic compositions do not couple with mass-dependent Ca or Ti isotope fractionation. One PLAC (7-644) has δ^{44} Ca/⁴⁰Ca +50 ± 20

 $^{^{10}}$ Following Ireland (1990), F_{Ti} is defined as $\Delta^{47}Ti$ deviations from the terrestrial $^{47}Ti/^{49}Ti$ (defined by Niederer and Papanastassiou, 1984). Note, subsequent publications report F_{Ti} is defined as $\Delta^{46}Ti$ deviations from the terrestrial $^{46}Ti/^{48}Ti$ (defined by Niederer and Papanastassiou, 1984).

which is resolved from the standard composition, but its mass-dependent Ti isotopic composition is the same as the standard (Ireland, 1990). This hibonite grain may, however, be related to HAL-type hibonites as it has a depletion in Ce (Ireland, 1990). Oxygen isotopic compositions¹¹ range from Δ^{17} O -28 to -17 ‰ (see Kööp et al., 2016a for this most recent compositional range). There are no Mg-isotopic effects indicating that PLACs did not reach high enough temperature to cause mass-dependent Mg isotope fractionation (Ireland, 1990). PLACs generally have low inferred initial 26 Al/ 27 Al indicating an absence of 26 Al (Ireland, 1988; Ireland, 1990; Kööp et al., 2016a).

There is a broad correlation between non-mass-dependent anomalies of ⁴⁸Ca, ⁵⁰Ti, and Δ¹⁷O. PLAC-like CAIs with the largest Δ¹⁷O values tend to possess the most anomalous ⁴⁸Ca and ⁵⁰Ti compositions, while those with the lowest Δ¹⁷O values have generally the least anomalous or normal ⁴⁸Ca and ⁵⁰Ti compositions (Kööp et al., 2016a). This may indicate a physical link between ⁴⁸Ca and ⁵⁰Ti carriers and a ¹⁶O-poor reservoir, where the initial Solar nebula was isotopically heterogeneous with respect to ⁴⁸Ca and ⁵⁰Ti carriers and this region was also ¹⁶O-poor (see Kööp et al., 2016a for details). A similar relationship is found in bulk meteorites (e.g., Yin et al., 2009; Warren et al., 2011; Dauphas et al., 2014a; Huang and Jacobsen, 2017). The correlation could be used to contrain the timing of the CO self-shielding process (Huang and Jacobsen, 2017). Alternatively, the correlation may imply local isotopic variability in the Solar nebula gas, or that PLAC sequilibrated in a gas of an evolving isotopic composition (e.g., Krot et al. 2012). Based on the low inferred initial ²⁶Al/²⁷Al compositions, the PLAC-forming region may have existed prior to the incorporated of ²⁶Al, indicating these may be the earliest formed objects in the Solar System (Kööp et al., 2016a).

3.1.1.5. SHIBs

Common refractory inclusion, in CM chondrites are "SHIBs" which are small (<160 µm) mineralogically complex grains dominated by hibonite and spinel. They possess variable TiO₂ hibonite concentrations <10 %, and clinopyroxene and refractory metal nuggets are trace phases in some SHIBs (Ireland, 1982; 'Kööp et al., 2016b, 2018a, and references therein). There are at least five SHIB morphologie (bladed, compact, massive, spherule, crystal; Ireland, 1990). The REE patterns of SHIB; are variable (ultrarefractory-deleted, ultrarefractory-enriched, or unfractionated REE patterns) and may correlate with morphology (e.g., Ireland, 1990).

Generally, SHIBs do not to possess large non-mass-dependent or mass-dependent Ca or Ti isotope effects. If these isotopes are variable in SHIBs, they are usually ± 10 % of the terrestrial value (Zinner et al., 1986; Ireland, 1990; Kööp et al. 2016b, 2018a). Kööp et al. (2016b) determined that SHIBs have a nearly constant Δ^{17} O value (\sim -23‰), and a generally high, near-canonical inferred initial 26 Al/ 27 Al although variability in 26 Al/ 27 Al exists (Ireland, 1990; Kööp et al., 2016b). Variability in 26 Al/ 27 Al may indicate variable 26 Al distribution in the SHIB-forming region (e.g., Fahey et al., 1987a; Ireland, 1988; 1990; Sahijpal et al., 2000; Liu et al., 2009). It has also been suggested, however, that variable 26 Al/ 27 Al in SHIBS is consistent

 $^{^{11}}$ Δ^{17} O refers to non-mass-dependent O isotopic compositions and is equivalent to δ^{17} O - 0.52* δ^{18} O. Δ 17O (Clayton, 1993).

with high temperature processing of refractory precursors that formed with initially approximately canonical ²⁶Al/²⁷Al ratios (Kööp et al., 2016b; Liu et al., 2019).

Generally non-anomalous Ca and Ti isotopic compositions and uniform ¹⁶O isotopic compositions of the SHIB forming region must be reconciled with their variable ²⁶Al/²⁷Al. This compositional profile may indicate that the SHIBs formed early in a region achieved isotopic homogeneity in O, Ca, and Ti isotopes prior to the homogenous distribution of ²⁶Al, such that these inclusions record the admixing of live ²⁶Al into the disk under variable thermal processing conditions (following Liu et al., 2012; see Kööp et al., 2016b). As noted by Kööp et al. (2016b), however, SHIB formation during variable addition of ²⁶Al would result in supracanonical and subcanonical ratios and a negative correlation between non-mass-dependent isotopic compositions and ²⁶Al is predicted. As these effects are not observed, Kööp et al. (2016b) cautiously concluded that the subcanonical ²⁶Al/²⁷Al compositions likely resulted from the resetting of the ²⁶Al-²⁶Mg system. If so, the homogeneity of the O isotopic compositions would imply that a homogeneous ¹⁶O-rich region persisted until at least ~0.7 Ma after formation of most CAIs, and SHIBs allow study of this phase of disk for ration.

3.1.2. Ca-Al-rich silicate refractory inclusions

Ca-Al-rich silicate CAIs are found mainly ($^{\prime}$ - 13 vol%) in carbonaceous chondrites CO > CV > CM > CK, in lower abundance ($^{\sim}$ 1 vc 1%) in CR > CI > CH > CB, and <0.1 vol% in ordinary, enstatite-, K-, and R- chondrites (K ot, 2014). The CAI primary mineralogy is similar to the first phases that are predicted to condense from a hot gas of Solar composition (e.g., Yoneda and Grossman, 1995; for review, see MacPherson et al., 2005 and MacPherson, 2014). The fractionated REE patterns of CA is 1. Alect multiple stages of evaporation and condensation of Solar nebular material in the disk (Taole 2). These observations, coupled with the ancient age of CAIs (e.g., 4567.30 ± 0.16 M i; Connelly et al., 2012), support the interpretation that CAIs are among the first condensates where in the protoplanetary disk. The most widely used CAI classification scheme is based on the compositions of large (mm to cm-scale) silicate-bearing (with minor hibonite) CA is from Allende because this meteorite is the most abundant in large CAIs and thus they have been studied in the most detail. According to the absolute and relative REE patterns of these CAIs, CAIs can be classified into one of six groups (Group I to Group VI; Mason and Taylor, 1982).

3.1.2.1. Silicate-bearing "regular" CAIs

Silicate-bearing inclusions, so-called "regular" CAIs, refer to those CAIs that are dominated by silicate mineralogy and with minor hibonite (Ireland et al., 1991). Many studies have investigated the Ca isotopic composition of mineral phases, acid leachates, and bulk rock samples of silicate-bearing CAIs from the CV and CM parent bodies (e.g., Niederer and Papanastassiou, 1979; Jungck et al., 1984; Niederer and Papanastassiou, 1984; Hinton et al., 1988; Weber et al., 1995; Sahijpal et al., 2000; Simon et al., 2009, 2017; Moynier et al., 2010a;

Huang et al., 2012; Chen et al. 2015; Amsellem et al., 2017; Bermingham et al., 2018; Schiller et al., 2018).

Refractory inclusions from Allende are considered to have condensed with approximately uniform $\Delta^{17}O$ values (\sim -23‰) and canonical $^{26}Al/^{27}Al$ ratios. Smaller CAIs from other meteorite groups (thermally unequilibrated ordinary chondrites and carbonaceous chondrites) record variable ^{16}O and heterogeneous ^{26}Al (Krot et al., 2012). In CAIs from CV and CR chondrites, small and generally positive $\epsilon^{48}Ca/^{44}Ca$ (<+10; e.g., Huang et al., 2012; Bermingham et al., 2018) and $\epsilon^{50}Ti/^{47}Ti$ (+7 to +12; e.g., Trinquier et al., 2009; Davis et al., 2018; Torrano et al., 2019) anomalies have been measured. Mass-dependent Ca isotopic compositions of CAIs are variable but predominantly light ($\delta^{44}Ca/^{40}Ca$ -14 to +6). Two Allende CAIs contain small excesses in $\epsilon^{40}Ca/^{44}Ca$ that correlate with excesses in $\epsilon^{50}Ti/^{47}Ti$ and $\epsilon^{135}Ba/^{136}Ba$, and deficits in $\epsilon^{142}Nd/^{144}Nd$ and $\epsilon^{144}Sm/^{154}Sm$ (Simon et al., 2009).

The non-mass-dependent Ca isotope anomalies may originate from the heterogeneous distribution of matter from either Type II or Type Ia supernovae (e.g., Simon et al., 2009; Moynier et al, 2010a; Huang et al; 2012; Dauphas et al., 2014a; Chen et al., 2015; Huang and Jacobsen, 2017; Bermingham et al., 2018). Yet to be ceter nined, however, are the number and type(s) of presolar ⁴⁸Ca carriers and the timing of their introduction into the Solar nebula.

Combining the mass-dependent Ca isotopic compositions with chemical signatures for the inclusions, Huang et al. (2012) observed the mass-dependent Ca isotopic compositions from bulk silicate-bearing CAIs correlate with 'EF abundance patterns. CAIs with Group II patterns tend to possess light δ^{44} Ca/ 40 Ca compositions compared to those with Group I patterns. Huang et al. (2012) interpreted these data to indicate that up to 3% of an ultrarefractory evaporation residue from a chondritic reservoir v/a, segregated prior to the formation of these CAIs. Bermingham et al. (2018) applied usis model to additional CAIs and AOAs samples from CV and CR meteorites. Some CAIs and AOAs followed the same trend documented by Huang et al. (2012). For those components that display unfractionated REE patterns, however, Bermingham et al. (2018) proposed they had display unfractionated REE patterns, however, Bermingham et al. (2018) proposed they had display unfractionated REE patterns, however, Bermingham et al. (2018) proposed they had display unfractionated REE patterns, however, Bermingham et al. (2018) proposed they had display unfractionated REE patterns, however, Bermingham et al. (2018) proposed they had display unfractionated REE patterns, however, Bermingham et al. (2018) proposed they had display unfractionated REE patterns, however, Bermingham et al. (2018) proposed they had display unfractionated REE patterns, however, Bermingham et al. (2018) proposed they had display unfractionated REE patterns, however, Bermingham et al. (2018) proposed they had display unfractionated REE patterns, however, Bermingham et al. (2018) proposed they had display unfractionated REE patterns and isotopic signatures were decoupled via disk or parent body alternation.

Although mass-dependent bulk CAI Ca isotope characteristics are largely consistent throughout the reported studies, Simon et al. (2017) observed intra-CAI Ca mass-dependent isotope zoning in an Allende CAI. These observations indicate that a refractory element can be isotopically fractionated at the scale of an inclusion. This possibility was suggested in the pioneering work by Niederer and Papanastassiou (1984) on Ca isotope studies in refractory inclusions; however, it was not confirmed until high precision mass spectrometry could be paired with micromilling techniques (Simon et al., 2017). Given these findings, isotopic variability within a meteorite component needs to be better documented to determine how accurately a bulk inclusion composition reflects the initial (presumably inner) CAI isotopic composition. For example, by expanding the database for isotope zonation studies to quantify the extent of isotopic variation for different elements from core to rim.

3.1.2.2. Silicate-bearing FUN CAIs

Silicate-bearing inclusions include unusual FUN CAIs. These refractory inclusions are mineralogically indistinguishable from normal CAIs and are only identifiable using their isotopic compositions that are highly fractionated (e.g., δ^{44} Ca/ 40 Ca -6 to +68, most displaying heavy compositions), display large non-mass-dependent isotopic variations (e.g., ϵ^{48} Ca/ 44 Ca -140 to +430), and have generally low inferred initial ²⁶Al/²⁷Al (e.g., Kööp et al., 2018b and references therein). Decoupling between the F and UN properties of FUN inclusions has been observed, where CAIs can show either highly mass-dependent fractionated compositions (F) or highly anomalous non-mass-dependent compositions (UN; e.g., PLACs and PLAC-like CAIs) (Wimpenny et al., 2014; Park et al., 2014, 2017; Kööp et al., 2015). These studies also found that the inferred initial ²⁶Al/²⁷Al compositions are canonical in 7 inclusions but are low in UN inclusions. Where oxygen data are available, it appears as thoug. CAIs with canonical ²⁶Al/²⁷Al ratios have approximately constant Δ^{17} O values (-23‰), whereas CAIs with low inferred initial 26 Al/ 27 Al ratios have variable Δ^{17} O values (Kööp et al., 2018b). Consequently, these highly variable compositions are likely a result of FUN-like in 'lus ons forming over an extended period of time sampling different stages of disk evolution and contributions from the parental molecular cloud (e.g., Kööp et al., 2018b; Simon et al., 2019).

3.1.3. Amoeboid olivine aggregate refract ry i iclusions

Amoeboid olivine aggregates are olivine (forsterite)-rich with trace Fe-Ni metal. They are irregularly shaped inclusions found in carbonaceous chondrites in similar abundances to CAIs (Grossman and Steele, 1976; for review the Krot et al., 2014). They are complex in their minor phase mineralogy, suggesting that they are aggregates of material that formed under a range of disk conditions (Ruzicka et al., 2012; MacPherson, 2014). This makes it difficult to link elemental and isotopic variations from bulk AOA analyses to their causation processes in the disk (Bermingham et al. 2018).

3.1.3.1 Ameboid olivine angregates

Ameboid olivine aggregates have not been extensively studied for Ca isotopic compositions. Bermingham et al. (2018) analyzed five AOAs from Allende and reported similar variations to many regular CAIs, with small ϵ^{48} Ca/ 44 Ca (<+10) isotope anomalies and generally light Ca mass-dependent isotopic compositions (δ^{44} Ca/ 40 Ca -0.95 to +0.72). There is no correlation between non-mass-dependent and mass-dependent Ca isotopic compositions. Type II REE pattern were recorded in some AOAs and this can correlate with light Ca isotopic composition; however, this is not pervasive. When these compositions are decoupled, it is likely a result of non-equilibrium condensation of the primary Ca-bearing mineral phases. Instead, bulk compositions may reflect an average REE and Ca isotopic composition of different mineral assemblages within the aggregate. Alternatively, the variable non-mass-dependent composition may indicate that AOAs formed over different regions or time periods of disk evolution. Isotopic

and chemical zonation studies and bulk sample analyses on additional AOAs are required to evaluate these interpretations.

3.2. Other meteorite components (chondrules, dark fragments, dark inclusions)

Recent studies report Ca isotopic compositions from bulk samples of chondrules, AOAs, dark fragments, and dark inclusions from CV, CM, R- and O-chondrites (Amsellem et al., 2017; Bermingham et al., 2018; Schiller et al., 2018). Following publications on refractory inclusions, these recent studies take a multipronged approach to sample analysis by comparing the mineralogy, REE compositions, and isotopic compositions of aggregates to provide chemical contexts in which to interpret the Ca isotopic composition of these complex sample types.

3.2.1. Chondrules

Chondrules are small (mm-sized) silicate-rich spherical objects commonly found in chondrites. They are generally considered to form from flast heating/cooling events in the disk over a period of up to ~3 Ma after t_0 (e.g., Pape et al., 20.9). Several chondrules from Allende have been studied for mass-dependent Ca isotopic effects, where Ca isotopic compositions can be either normal, slightly heavy, or slightly light relative to Earth (δ^{44} Ca/ 40 Ca +0.30 to +1.59) (Amsellem et al., 2017; Simon et al., 2017; Bermingan m et al., 2018). Bermingham et al. (2018) noted that some Ca mass-dependent isotopic compositions do not correlate with REE patterns, which was interpreted to indicate the conditions that set the chemical signatures of the chondrules were not responsible for determining their Ca isotopic compositions. Three chondrule compositions may preserve the relationship between REE and Ca mass-dependent isotopic composition, where chondrules with Group I REE patterns and moderate Ca isotope fractionation accreted both the condensate and the ultrarefractory residue.

Non-mass-dependent Ca isotopic compositions have been obtained from chondrules in CV, R- and O-chondrites (Benningham et al., 2018; Schiller et al., 2018). In general, the non-mass-dependent Ca isotopic compositions of chondrules are variable and exhibit small ϵ^{48} Ca/ 44 Ca (<+12) isotopic anomalies. Schiller et al. (2018) suggested that the variation in non-mass-dependent Ca isotopic composition may indicate a rapid change in the composition of the material of the protoplanetary disk during the ~1 Ma time period over which ordinary chondrite derived chondrules formed. Future studies combining age determination and Ca isotope analyses will be critical in evaluating this interpretation.

3.2.2. Dark fragments and dark inclusions

Dark fragments from R chondrites are considered to be among the most primitive R-lithologies (Bischoff et al., 2011). Dark inclusions from Allende (CV3) are lithic chondritic clasts that may have formed in the disk (Kurat et al. 1989) or on the CV parent body (Krot et al., 2000a). Neither the dark fragments nor the dark inclusions possess variations in non-mass-dependent Ca isotopic compositions (Bermingham et al., 2018). These samples, however, display slightly heavy Ca isotopic compositions (δ^{44} Ca/ 40 Ca +1.26 to +1.33), indicating that they likely

do not sample materials with highly variable Ca isotopic compositions and thus are not aggregates of direct nebular condensates. The Ca isotopic compositions support the interpretation that the inclusion formed *in situ* on the parent body as a variably altered fragment of the CV3 parent body lithology (Krot et al., 2000a). From Bermingham et al. (2018), the Ca isotopic composition of some dark inclusions may have been reset during parent body-based aqueous alteration events after lithification and aggregation of the inclusion. During alteration, diffusion-driven Ca isotope exchange reactions (for details, see Krot et al., 2000b) between the surrounding matrix and the inclusion may have occurred and resulted in the formation of Ca-rich rims. During these reactions, Ca isotopic compositions would become progressively lighter in the rim-deposits (see Section 2.2 for details on Ca isotope effect during diffusion). Isolation of this inclusion from the matrix resulted in the removal of rim material and thus likely biased the bulk Ca isotopic composition recorded to the heavier core composition. Future chemical and isotopic zonation studies that pair high precision mass spectrometry with micromilling techniques (following Simon et al., 2017) would provide the means to text it is hypothesis and constrain the process(es) that fixed the Ca isotopic composition of Allena dark fragments.

3.3. Synthesis of meteorite component Ca isotopic dat

Reconciling chemical and isotopic data from all types of chondrite components to produce a coherent model of protoplanetary discrevolution is challenging because many studies do not consistently generate coupled chemical and multi-isotopic (e.g., Ca, Ti, O, Mg-Al, and REE) datasets. To date, the chemical and iscrepic data reviewed above indicates that the disk was isotopically and chemically heterogeneous over space and time.

Bermingham et al. (2018) attemped to constrain the origin of Ca isotopic variations in the disk by contrasting the Ca mags-dependent and non-mass-dependent isotopic composition of different components. Non-mass-dependent isotope effects are generally considered to be the result of poorly mixed presoner carrier phases throughout the disk; however, debate remains regarding the process by which these grains became heterogeneously distributed in the disk. It has been posited that non-mass-dependent Ca isotopic heterogeneity is the result of two-component mixing of an anomalous endmember component (e.g., Type Ia or Type II supernova) with a Solar component (Simon et al., 2009; Chen et al., 2011; Huang et al., 2012; Dauphas et al., 2014a; Chen et al., 2015; Wasserburg et al., 2015; Huang and Jacobsen, 2017).

Thermal processing of multiple carrier phases has been proposed as an alternative interpretation (Schiller et al., 2015). If high enough temperatures were reached during thermal processing events, preferential removal of light Ca isotopes would have occurred, leaving an isotopically heavy and isotopically anomalous ^{48}Ca residue (Bermingham et al., 2018). This effect may be apparent when comparing non-mass-dependent and mass-dependent Ca isotopic compositions, where heavy isotope signatures would be coupled with more anomalous non-mass-dependent compositions, thus a positive $\delta^{44}\text{Ca}/^{40}\text{Ca}$ and $\epsilon^{48}\text{Ca}/^{44}\text{Ca}$ correlation was predicted.

A recent investigation of this relationship indicated that mass-dependent and non-mass-dependent Ca isotopic compositions in nine "regular" silicate-bearing CAIs were not linearly coupled, although light δ^{44} Ca/ 40 Ca compositions were generally coupled with enrichments in ϵ^{48} Ca/ 44 Ca (Bermingham et al., 2018). From a preliminary investigation (see **Fig. 3**), a simple correlation is absent when comparing Ca isotopic compositions of meteorite components. Davis et al. (2018) found no relationship between mass-dependent and non-mass-dependent fractionation for Ti isotopes in 46 Allende CAIs, even though there is a significant range in both mass-dependent and non-mass-dependent fractionation among CAIs. Thus, the lack of such a ubiquitous relationship for Ca isotopes is perhaps not surprising, but the reason remains unclear. To determine the relationship between mass-dependent and non-mass-dependent isotopic compositions coupled datasets are required. Extending this test to the chondrite components is most judiciously done by comparing datasets that report coupled no sedependent and non-mass-dependent data from the same samples, using the same fractionation laws and normalization schemes, and data collected using similar anglytical methods.

Similar to the trend noted by Ireland (1990), the α is a continuum in the degree of ϵ^{48} Ca/ 44 Ca heterogeneity between CAIs-types: PLAC/F IN > hibonite-bearing spherules > SHIB > regular CAIs > AOAs/chondrules. Additionally, sy tematic relationships are apparent among chondrite components. (1) PLACs record the post extreme enrichments and depletions in ϵ^{48} Ca/ 44 Ca compositions of Solar System-derived materials, yet mass-dependent Ca isotope fractionation is absent. (2) FUN (including F, UN) and HAL-type possess large excesses and depletions in ϵ^{48} Ca/ 44 Ca and these inclusion, are predominantly heavy in mass-dependent Ca isotopic composition. (3) Hibonite-bearing spherules generally record large excesses in ϵ^{48} Ca/ 44 Ca compositions, whereas mass-dependent Ca isotope fractionation is not evident. (4) SHIBs possess moderate (6 to 10 times less anomalous than PLACs) non-mass-dependent Ca isotope anomalies; however, some PLACs have similar Ca isotopic compositions as SHIBs. (5) Silicate-bearing "regular" CAIs are dominated by relatively small excesses in ϵ^{48} Ca/ 44 Ca which are commonly coupled with high mass-dependent Ca isotopic compositions.

The absence of resolved mass-dependent Ca isotope fractionation in PLACs and microspherules suggests that if thermal processing event(s) produced non-mass-dependent Ca isotope anomalies, they did not concurrently establish the observed mass-dependent effects. The fact that in some FUN CAIs, large excesses or depletions in ε^{48} Ca/ 44 Ca are coupled with large heavy mass-dependent fractionation suggests there may be a causal relationship between the two effects, but this is not ubiquitous because the relationship is not seen in all FUN, F, or UN CAIs. The Ca isotope systematics change in regular CAIs where positive ε^{48} Ca/ 44 Ca anomalies are predominately coupled with light Ca isotopic compositions (**Fig. 3b**). Given that "regular" CAIs have the light Ca effects, it is possible that these CAIs formed from the fractionated gas that was enriched in light Ca isotopes imparted from earlier fractionation.

Studies that couple Ca isotopic compositions with chemical and isotopic data of other elements which record thermal processing events in the disk (e.g., REE, and O-, Al- and Ti-isotopic data) are required to determine how the Ca isotopic composition of meteorite

components originate. This multi-element approach to analyzing chondrite components will also provide constraints that directly inform the following fundamental questions in cosmochemistry: (1) what were the combination and timing of stellar precursors into the Solar nebula; (2) what is the significance of non-mass-dependent isotopic compositions of refractory inclusions regarding mixing processes and location of these reservoirs in the disk; and (3) are non-mass-dependent compositions linked to mass-dependent isotopic compositions?

4. Planetary building blocks: bulk chondrites and achondrites

The building blocks of the Earth may be found in our meteorite collection; thus, studying meteorites in detail can provide insight into how a life-bearing planet evolved. This section surveys constraints provided by Ca isotopes in bulk chondrites, and achondrites, including samples from the Moon and Mars.

4.1 Introduction to bulk meteorite samples

Bulk meteorites are useful for evaluating the genetic relationships between parent bodies that formed from isotopically distinct reservoirs in the dis's (e.g., Chambers, 2001; Drake and Righter, 2002; O'Brien et al., 2006; Warren, 2011). Lotopic variations among bulk meteorites can be used to constrain the chemical nature of Eurin's accretionary assemblage and to link this assemblage to specific formation locations within the protoplanetary disk.

Chondrites have been divided into fist act classes that are defined primarily by their bulk chemical compositions, and secondarily by parameters such as mineralogy, oxygen isotopic composition, and chondrule abundance (Prearley and Jones, 1998; Weisberg et al., 2006; Krot et al., 2014). Most chondrites fall into one of three main classes: carbonaceous chondrites, ordinary chondrites, and enstatite chondrites. The cause of differences among classes is interpreted to reflect distinctive accretion location; within the disk (Wasson and Kallemeyn, 1988; Rubin and Wasson 1995; Wood, 2005; Payanond et al., 2009). CI chondrites are the most chemically primitive meteorites as they be compositions—volatile elements excluded—similar to the Solar photosphere (e.g., Orgi eil CI; Anders and Grevesse, 1989; Palme et al., 2014; Lodders, 2020). Carbonaceous chondrites, however, are by no means unaltered, as some have undergone extensive aqueous alteration (e.g., Zolensky and McSween, 1988; Brearley, 2006). Some members of the carbonaceous chondrite group contain the highest volatile element content compared to the Earth (e.g., Bland et al., 2005); thus, they are inferred to have originated from asteroidal parent bodies that accreted far from the sun (Gradie and Tedesco, 1982).

Ordinary chondrites are also rich in volatiles compared to the Earth, but to less so than most carbonaceous chondrites (Palme et al., 2014; Scott and Krot, 2014;); they feasibly derive from parent bodies formed in the inner asteroid belt (Binzel et al., 1996). In enstatite chondrites, iron exists mainly in its metallic form or as a sulfide, in contrast to carbonaceous and L- and LL-type ordinary chondrites, where Fe is mostly present in oxides. The high metal content and low oxygen fugacity of enstatite chondrites indicates these meteorites formed in reduced part of the

disk, possibly in the inner Solar System (Krot et al., 2014; Palme et al., 2014; Scott and Krot, 2014).

Achondrite meteorites sample the silicate crust and mantle of parent bodies that reached temperatures high enough to induce partial or wholesale melting (including 4-Vesta, the ureilite parent body, the Moon, and Mars). As such, achondrites present an opportunity to study the Earth's accretion of planetesimals that had already differentiated to some degree (e.g., Kleine et al., 2005; Kruijer et al., 2014). Chemical and isotopic analyses along with dynamical simulations have suggested that the parent bodies of achondrites possibly accreted earlier and closer to the Sun than the parent bodies of chondrites and some iron meteorites (e.g., Wasson and Wetherill, 1979; Grimm and McSween, 1993; Kleine et al., 2005; Bottke et al., 2006; Warren, 2011). Thus, through the analysis of achondrites and chondrites different regions of the protoplanetary disk can be probed.

Most current models propose that the Earth accreted from a heterogeneous mixture of chondritic and achondritic precursors that formed at different heliocentric distances; however, the relative proportion of each precursor type remains devoted (e.g., Drake and Righter, 2002; Fitoussi et al., 2016; Dauphas et al., 2017; Liebske and han, 2019). It has been argued that reduced, non-carbonaceous material (including achondrite) dominated the early part of Earth's main accretion history, while more oxidized, volutile rich carbonaceous chondrite-like material accreted toward the end of Earth's formation (e.g., Schönbächler et al., 2010; Rubie et al., 2015; Budde et al., 2019; Grewal et al., 2019; Hopp et al., 2020). It is feasible that the transition occurred at the time of the Moon-forming appact (e.g., Schönbächler et al., 2010). To a first approximation, however, Earth's bulk relemental composition is chondritic as the relative proportions of non-volatile elements in a central composition in chondrites (the so-called "chondritic Earth" model; Larimer, 1271; Kargel and Lewis, 1993; Palme and O'Neill, 2014).

4.2 Non-mass-dependent Ca is to ic variations among chondrite groups

The discovery of 1 a 1 2° Xe and Ne isotopic anomalies in carbonaceous chondrites (Reynolds and Turner, 1964; 3lack and Pepin, 1969; Lewis et al., 1975) and 17 O heterogeneity among meteorites and their components (Clayton et al., 1973) challenged the paradigm that the Solar System formed out of an initially homogeneous gas cloud (e.g., Cameron, 1962). Because these anomalies could not be linked to fission, spallation or Solar wind implantation, they were interpreted to derive from stellar lineage and, therefore, predate the Solar System. The subsequent identification of diamond (Lewis et al., 1987), silicon carbide (Bernatowitz et al., 1987; Zinner et al., 1987), and graphite (Amari et al., 1990) presolar grains as the host phases of noble gas anomalies provided evidence that presolar isotopic diversity had survived the nebula phase and was preserved in meteorites.

The idea of early Solar nebula heterogeneity was further strengthened by the detection of non-mass-dependent isotopic effects in major rock-forming elements, including Ca, in CAIs and other refractory chondrite components (e.g., Lee et al., 1978, 1979; Niederer and Papanastassiou, 1984; see **Section 3**). Technical refinements and improvements in analytical sensitivity of TIMS

and MC-ICP-MS permitted expansion of sample types that could be measured. This resulted in a shift of focus from refractory inclusions to bulk meteorites. Detection of non-mass-dependent effects in bulk meteorites showed that the heterogeneous distribution of Ca isotopes was preserved at the planetary scale (Simon et al., 2009; Chen et al., 2011; Dauphas et al., 2014a; Bermingham et al., 2018). This demonstrated the utility of Ca isotopes for probing the genetic relationship between meteorite groups, the Earth, and other rocky planets, because they ostensibly formed in (isotopically) distinct regions of the disk (Dauphas, 2017).

Until rather recently, only two bulk Ca isotopic measurements had been published, both on Allende (Niederer and Papanastassiou, 1979, 1984). Anomalous ϵ^{46} Ca/ 44 Ca (-140) and ϵ^{48} Ca/ 44 Ca (-29) were detected by Niederer and Papanastassiou (1979) but not Niederer and Papanastassiou (1984). Later, Simon et al. (2009) measured ϵ^{40} Ca 44 Ca and ϵ^{43} Ca/ 44 Ca variations in a suite of enstatite, ordinary, and carbonaceous chondrites. In this study, measurement uncertainties are generally too large to resolve chondrite com, octions from Earth; however, carbonaceous chondrites Murray (CM2) and Vigarano, and ordinary chondrites St. Severin (LL6) and Dhajala show ϵ^{40} Ca/ 44 Ca and ϵ^{43} Ca/ 44 Ca enrichments of +0.3 to +2.3 relative to Earth (**Fig. 4**). These data indicate that the isotopic reservoid sampled by carbonaceous and ordinary chondrites are distinct from the dominant composition of Earth's building blocks. Moynier et al. (2010a) corroborate these results by showing that Oha'ala is distinct from Earth, with anomalous ϵ^{40} Ca/ 44 Ca \sim +2 and ϵ^{43} Ca/ 44 Ca \sim +0.5. In addition to data for ϵ^{40} Ca/ 44 Ca and ϵ^{43} Ca/ 44 Ca, Moynier et al. (2010a) present data for ϵ^{46} Ca/ 44 Ca and ϵ^{40} Ca/ 44 Ca can not be resolved, but Dhajala, Murray, and Vigarano have distinct ϵ^{48} Ca/ 44 Ca from Earth with enrichments of up to +4.

Dauphas et al. (2014a) identily enrichments in ϵ^{48} Ca/⁴⁴Ca between +2 to +4 in CI, CO, and CV chondrites. The authors also measure ordinary chondrites (LL, L and H); however, these are indistinguishable from Earth Likewise, enstatite chondrites Adhi Kot (EH) and Jajh (EL) are also within analytical uncertainty of Earth (**Fig. 4**). The results of Huang and Jacobsen (2017) support these findings as they and no discernable ϵ^{40} Ca/⁴⁴Ca or ϵ^{43} Ca/⁴⁴Ca anomalies in a suite of nine chondrites (Ci, Ci, CV, L, H, and EH) relative to Earth at the \pm 1 and \pm 2 ϵ -unit levels, respectively. This study does not detect ϵ^{48} Ca/⁴⁴Ca anomalies in enstatite chondrites and ordinary chondrites, though all carbonaceous chondrite types show ϵ^{48} Ca/⁴⁴Ca excesses between +2 and +3. Yokoyama et al. (2017) present data for seven ordinary chondrites, four of which display small but resolvable ϵ^{40} Ca/⁴⁴Ca excesses, where the largest anomaly is recorded by Bhola (LL3) (ϵ^{40} Ca/⁴⁴Ca +2.5).

By obtaining an order of magnitude higher precision than previous studies, Schiller et al. (2015) report non-mass-dependent 43 Ca/ 44 Ca, 46 Ca/ 44 Ca, and 48 Ca/ 44 Ca effects in ordinary and carbonaceous chondrites. One ordinary chondrite (Bovedy, L3) records ϵ^{43} Ca/ 44 Ca and ϵ^{46} Ca/ 44 Ca compositions that are unresolvable from Earth but have a ϵ^{48} Ca/ 44 Ca depletion of -0.35. Ivuna (CI) is enriched in ϵ^{43} Ca/ 44 Ca (+0.11), ϵ^{46} Ca/ 44 Ca (+0.96), and ϵ^{48} Ca/ 44 Ca (+2.06) relative to Earth. Schiller et al. (2018) also show that the ϵ^{48} Ca/ 44 Ca compositions of ordinary and carbonaceous chondrites (including CI, CM, CR, C2-ungrouped) do not overlap with that of

Earth. The ε^{48} Ca/ 44 Ca depletion in ordinary chondrites (-0.35 to -0.25) and excess in carbonaceous chondrites (+2.06 to +3.14) are similar to that reported in Schiller et al. (2015).

4.2.1 Earth's building blocks constrained by non-mass-dependent Ca isotopes in chondrites

That the Ca isotopic compositions of carbonaceous chondrites and ordinary chondrites are anomalous relative to Earth indicates that these meteorite types likely do not make up a significant proportion of Earth's precursor material. In contrast, the lack of non-mass-dependent Ca isotopic effects in enstatite chondrites suggests that the Earth and the enstatite chondrite parent body formed from a similar isotopic reservoir in the disk. These findings place Ca on the growing list of elements that display isotopic similarity between Earth and enstatite chondrites but not between the Earth and other meteorite groups—this includes O¹², Si, Ni, Ti, Cr, Sr, Zr, Ru, Ba, and Mo (O: Clayton, 2004; Ni: Regelous et al., 2008; Ti. Trinquier et al., 2009; Cr: Qin et al., 2010; Sr: Moynier et al., 2012; Zr: Akram et al., 2015; Pu. Ticher-Gödde et al., 2015; Ba: Bermingham et al., 2016; Mo: Worsham et al., 2017).

Using models based on mixing calculations, Daupha's et al. (2014a) and Dauphas (2017) demonstrated that Earth's Δ^{17} O, ϵ^{48} Ca, ϵ^{50} Ti, ϵ^{54} Cr, ϵ^{64} Ti, and ϵ^{92} Mo isotopic composition cannot be reproduced unless the proportion of enstable chondrites in bulk Earth was >90%. Accretion of significantly less enstatite chondrite matrial yields a mismatch between the Earth and calculated isotope mixtures for one or more of the elements. The non-mass-dependent O, Ca, Sr, Ti, Cr, Ni, Zr, Ru, Ba, and Mo isotopic similarity between the Earth and enstatite chondrites supports the interpretation that the Earth primarily accreted material with approximately the same isotopic composition as that sampled by enstatite chondrites (Dauphas et al., 2014a; Dauphas, 2017).

How closely enstatite chor dries are related to Earth, however, has long been the subject of debate (e.g., Javoy and Pineza, 1983; Javoy, 1995; Javoy et al., 2010). The discussion focuses on the fact that, though enstatic chandrites and Earth resemble each other isotopically, they have very dissimilar elemental compositions. In particular, enstatite chondrites are depleted in FeO, enriched in volatiles, and have Si/Mg ratios higher than BSE (Wasson and Kallemeyn, 1988; Allègre et al., 1995). It may be that Earth and enstatite chondrites formed from the same parental nebular reservoir but experienced different condensation processes (Jacobsen et al., 2013; Dauphas et al., 2014a; Dauphas, 2017; Huang et al., 2017). Experimental data and numerical modelling that simulates the condensation processes responsible for the observed differences in element composition is required to evaluate the validity of this hypothesis. Presently, however, non-mass-dependent Ca isotopic data support the hypothesis that the Earth formed primarily from material similar to enstatite chondrites.

4.3. Mass-dependent variation among chondrite groups

¹² Proposals for the origin of meteoritic O isotopic variations now include photochemical effects (Clayton 2002) and non-mass-dependent chemical effects (Thiemens and Heidenreich 1983).

Early studies determined that the δ^{40} Ca/ 44 Ca signatures of bulk carbonaceous, ordinary, and enstatite chondrites (represented by CI, H6, and EH types: Russell et al., 1978; CV: Niederer and Papanastassiou., 1979, 1984) were indistinguishable from Earth, with no systematic variation in 40 Ca/ 44 Ca by chondrite type. More recent data indicates that some 44 Ca/ 40 Ca variation does, in fact, exist among chondrite groups, and between chondrite groups and Earth, at the <0.1% level of precision (**Fig. 5**). Specifically, carbonaceous chondrites display δ^{44} Ca/ 40 Ca_{CI} +0.42 to +1.13, δ^{44} Ca/ 40 Ca_{CM} +0.55 to +0.84, δ^{44} Ca/ 40 Ca_{CO} +0.77 to +1.19, δ^{44} Ca/ 40 Ca_{CV} +0.10 to +0.78, ordinary chondrites display δ^{44} Ca/ 40 Ca_{LL,L,H} +0.91 to +1.16, and enstatite chondrites display δ^{44} Ca/ 40 Ca_{EH,EL} +0.90 to +1.54 (Simon and DePaolo, 2010, Valdes et al., 2014, Schiller et al., 2015; Amsellem et al., 2017, Huang and Jacobsen, 2017, Simon et al., 2017). Notably, analytically resolvable differences in δ^{44} Ca/ 40 Ca have also been resorted in the same meteorite sample measured by different groups—for example, in Allen of Murchison (CM2), Orgueil, Abee (EH4), Indarch (EH4), and Qingzhen (EH3) (Valdes et al., 2014; Bermingham et al., 2018).

Generally, studies agree that carbonaceous chondries are enriched in light Ca isotopes relative to Earth and ordinary chondrites have 44 Ca/ 40 C a cc mpositions that are indistinguishable from Earth (Simon and DePaolo, 2010; Huang and Jacobson, 2017; Valdes et al., 2014; Schiller et al., 2015; Bermingham et al., 2016; Amselle n et al., 2017; Simon et al., 2017). There is disagreement, however, on whether enstatit conondrites also possess identical 44 Ca/ 40 Ca compositions to Earth. Some studies, e.g., Va'des et al. (2014) (δ^{44} Ca/ 40 Ca_{EL,EH} +0.90 to +1.01), Amsellem et al. (2017) (δ^{44} Ca/ 40 Ca_{EL,EH} +0.90 to +0.96), reported no analytically resolvable Ca isotope fractionation between Earth and enstatite chondrifes. In contrast, Simon and DePaolo (2010) reported that enstatite chondrites have δ^{44} Ca/ 40 Ca_{EL}, compositions up to +0.5 higher than that of the Earth. The findings by Simon and DePaolo (2010) also stand contrary to data for other multi-isotopic major elements, such as O (e.g., Clay on et al., 2003), Fe (e.g., Poitrasson et al., 2004; Craddock and Dauphas, 2011; Wang et al., 2014), Mg (e.g., Teng et al., 2010), and Si (e.g., Savage and Moynier, 2013), which in lica e that enstatite chondrites and Earth are isotopically uniform.

4.3.1 The origin of mass-dependent Ca isotope variability between and within chondrite groups

It has been suggested that the variability between and within chondrite groups was established by a heterogeneous distribution of primitive solids with variable δ^{44} Ca/ 40 Ca compositions imparted during early disk processing (see **Section 3**) (Simon and DePaolo, 2010; Valdes et al., 2014; Huang et al., 2017; Bermingham et al., 2018). For example, the light δ^{44} Ca/ 40 Ca signatures of bulk carbonaceous chondrites may reflect an overabundance of CAIs that are isotopically light as a result of non-equilibrium condensation (Simon and DePaolo, 2010) or ultrarefractory evaporative residue loss (Huang et al., 2012; Bermingham et al., 2018). Notably, however, CI chondrites do not contain obvious CAIs but do have light δ^{44} Ca/ 40 Ca signatures (Valdes et al., 2014; Huang and Jacobsen, 2017; Bermingham et al., 2018). Thus, the isotopically light Ca compositions of bulk carbonaceous chondrites cannot be exclusively

attributed to CAI abundance, and likely reflects several generations of early nonequilibrium solid-gas fractionation including some prior to CAI formation (Simon and DePaolo, 2010). Neither can chondrules, which on average have δ^{44} Ca/ 40 Ca signatures identical to Earth, exclusively account for the light, variable δ^{44} Ca/ 40 Ca signatures in bulk carbonaceous chondrites.

As a fluid-mobile element, Ca can be strongly chemically fractionated among alteration products in chondrite matrices (Brearley, 2006); thus, it is possible that parent body alteration and/or terrestrial weathering produced mass-dependent Ca isotope fractionation effects in Cabearing chondrite phases. In this case, meteorites that variably sample phases modified by parent body alteration and/or terrestrial weathering may record isotopic differences between and within chondrite groups or conceal isotopic signatures imparted by the heterogeneous distribution of primitive solids.

Bermingham et al. (2018) suggested that if parent body aqueous alteration played a significant role in establishing δ^{44} Ca/ 40 Ca differences among chondrites, meteorites from chondrite groups that are substantially affected by love-temperature alteration (e.g., CI chondrites) would display greater δ^{44} Ca/ 40 Ca variability that those chondrite groups less affected (e.g., CO chondrites; Brearley, 2006). Indeed, CI chondrite (δ^{44} Ca/ 40 Ca_{CI} +0.42 to +1.13) show more Ca isotopic variation than CO chondrites (δ^{44} Ca/ 40 Ca_{CI} +0.77 to +1.19), thereby supporting the interpretation that parent body alteration plays a role in modifying the bulk δ^{44} Ca/ 40 Ca composition.

It is less clear if aqueous alteratio as a result of terrestrial weathering has a measurable effect on the bulk δ^{44} Ca/ 40 Ca compositions of chondrites. For example, Bermingham et al. (2018) noted that some oldhamite grains in MacAlpine Hills 88136¹³ display evidence of aqueous alteration (Lundberg et al., 1964), and suggested that alteration of oldhamite may have overprinted the primary Ca is once signature imparted during accretion. Although a heterogeneous distribution of isotopically heavy oldhamite cannot be the sole cause of Ca isotopic variation in chondrite 5 oups, it may cause Ca isotope variability within a group. Prior to this, it had been proposed that errestrial alteration of oldhamite, which is highly soluble and easily aqueously mobilized, r ay result in its preferential dissolution and the removal of light Ca isotopes, resulting in an anomalously heavy oldhamite, and therefore bulk, δ^{44} Ca/ 40 Ca composition (Bermingham, 2011, Valdes et al., 2014). Valdes et al. (2014), however, dismiss this interpretation because the heavy δ^{44} Ca/ 40 Ca signatures for oldhamite obtained in their Indarch leaching experiment were not fractionated enough from the bulk composition to account for the magnitude of the MacAlpine Hills 88136 offset from Earth as reported by Simon et al. (2010). Conversely, according to the ab initio calculations of Huang et al. (2019), oldhamite should have lighter Ca isotope signatures compared to bulk under equilibrium conditions, which is in disagreement with the results of Valdes et al. (2014).

Further investigation of Ca isotopic variability in bulk samples as a consequence of fluid alteration of oldhamite (and other Ca-bearing phases) is necessary to constraining parent body

 $^{^{13}}$ MacAlpine Hills 88136 is the sample that provides the upper limit for the $\delta^{44} \text{Ca}/^{40} \text{Ca}$ +0.5 offset of enstatite chondrites from Earth (Simon et al., 2010).

compositions. As reported, bulk δ^{44} Ca/ 40 Ca data suggest that the Earth may have accreted primarily from precursors with a composition similar to that of enstatite and/or ordinary chondrites; however, future studies should carefully evaluate for the effects of variably sampling isotopically heterogeneous primitive solids when using the Ca isotopic compositions of bulk meteorites to trace planetary building blocks.

4.4. Non-mass-dependent and mass-dependent Ca isotopic variation among achondrites, the Moon, and Mars

4.4.1. Achondrites

Mass-dependent and non-mass-dependent Ca isotopic data for bulk achondrites are presented in **Figs. 4 and 5**. Studies are in agreement that bu.' angrites, aubrites, ureilites, winonaites, and presumed differentiation products of 4-Ve_{2.00} (cucrites, diogenites) have $^{40}\text{Ca}/^{44}\text{Ca}$, $^{42}\text{Ca}/^{44}\text{Ca}$, $^{43}\text{Ca}/^{44}\text{Ca}$, and $^{46}\text{Ca}/^{44}\text{Ca}$ compositions that are indistinguishable from Earth at a precision of <0.2‰ (Simon and DePaolo, 2010; Val les et al., 2014; Schiller et al., 2015; Schiller et al., 2018). These achondrite groups chibit uniform non-mass-dependent $^{40}\text{Ca}/^{44}\text{Ca}$, and $^{46}\text{Ca}/^{44}\text{Ca}$ compositions that are not analytically resolved from Earth (Simon et al., 2009; Chen et al., 2011; Dauphas et al., 2014a; Schiller et al., 2015; Huang and Jacobsen, 2017; Yokoyama et al., 2017; Schiller et al., 2018). All primitive achondrite groups studied to date, however, have well-resolved ⁴⁸Ca deficits (ε⁴⁸Ca/⁴⁴Ca -1 to -2) relative to Earth. Achondrite groups vary in degree of Ca i otope heterogeneity, with group-average ⁴⁸Ca deficits increasing in the order of eucrites > angrites - diogenites > ureilites (Chen et al., 2011; Dauphas et al., 2014a, Schiller et al., 2018).

The cause of ε^{48} Ca/⁴⁴Ca het r/g neity is debated. In bulk achondrite groups, it may derive from variable mixing between material of Solar composition with isotopically anomalous material ejected from Type Ia or electron-capture supernova explosions (e.g., Simon et al., 2009; Moynier et al., 2010a; Chen e. al., 2011; Dauphas et al., 2014a; Huang and Jacobsen, 2017; Bermingham et al., 2018). Attendatively, ε^{48} Ca/⁴⁴Ca anomalies may be indicative of selective and variable unmixing between two homogeneously distributed dust reservoirs via sublimation of thermally unstable, isotopically anomalous presolar carriers (Schiller et al., 2015). Regardless of the cause, it is evident that, despite unfractionated mass-dependent Ca isotopic compositions of bulk achondrites from that of Earth, planetary formation and differentiation processes were ineffective in fully homogenizing the Ca isotopic composition of the Solar System.

4.4.2. The Earth-Moon system

The canonical giant impact theory for the formation of the Moon proposes that a Marssized body (Theia) collided with the proto-Earth and ejected material into an Earth-orbiting disk, which subsequently re-accreted to form the Moon (e.g., Hartmann and Davis, 1975; Cameron and Ward, 1976). A long-standing question concerns the composition of the impactor. Early impact models predicted the Moon to be largely derived from the impactor (e.g., Cameron, 2000; Canup and Asphaug, 2001, 2012); however, in this scenario it is remarkable that the O, Si, Ti,

Mg, and Cr isotopic compositions of Earth and the Moon are indistinguishable, within analytical uncertainty (e.g., Lugmair and Shukolyukov, 1998; Wiechert et al., 2001; Spicuzza et al., 2007; Fitoussi et al., 2010; Oin et al., 2010; Armytage et al., 2011; Warren, 2011; Zhang et al., 2012; Sedaghatpour et al., 2013; Young et al., 2016; Bonnand et al., 2016; Mougel et al. 2017). Given the variability exhibited by these isotopes among other planetary bodies, the similarity between the Earth and the Moon is significant. This similarity has been used to support the interpretation that the proto-Earth and the impactor formed from the same reservoir of material located in the inner part (≤1.5 AU) of the disk (Jacobsen et al., 2013; Dauphas et al., 2014b), or that the Moon was primarily formed from the proto-Earth (Zhang et al., 2012). Alternatively, the proto-Earth and the impactor may have been compositionally distinct, but this would require, for example, turbulent mixing and equilibration in the aftermath of the fiant impact to isotopically homogenize the system (Pahlevan and Stevenson, 2007; Young et al., 2016). Recently, numerical calculations based on a fast-spinning Earth and a high chergy impact (Cuk and Stewart 2012; Lock et al., 2018) have predicted isotopic similarity betyeen the Earth and Moon as a consequence of the Moon's direct condensation from a comogenized disk of vapor deriving primarily from Earth's mantle (Lock et al., 2018; see refer ent review by Lock et al., 2020).

The number of studies that have published Ca isotopic data for bulk lunar samples is still limited (**Figs. 4 and 5**), but the few available data ρ vints show that the Moon and Earth have identical mass-dependent and non-mass-dependent to a isotopic compositions. In 15 lunar basalts (meteoritic, as well as from Apollo 11, 12–14 and 15), Simon and DePaolo (2010), Valdes et al. (2014), and Simon et al. (2017) find $\delta^{44}Ca$. (Apollo 15) Simon and DePaolo (2010), Valdes et al. (2014), and Simon et al. (2017) find $\delta^{44}Ca$. (Apollo 16) Apollo 17 and low-Ti (Apollo 12, 14, 15) basalts. Three green glass samples exhibit no resolvable in actionation from lunar basalts and Earth. One anorthosite, however, Dhofar 026, is isotopic ally light relative to Earth (Schiller et al., 2018).

Non-mass-dependent Ca isotopic data has only been reported for four basaltic meteorites and one Apollo 16 anorthosite. Neither the ⁴⁸Ca/⁴⁴Ca compositions measured in basalts (Schiller et al., 2018) nor the ⁴⁰Ca/⁴⁴Ca, ⁴³Ca/⁴⁴Ca and ⁴⁸Ca/⁴⁴Ca compositions measured in the anorthosite show any fractionation from Earth within analytical uncertainty.

What the Ca isotopic similarity between the Earth and Moon indicates about their genetic relationship is not clear. It is yet to be understood if the data best support (i) the formation of the Moon predominantly from proto-Earth material (Zhang et al., 2012), (ii) the isotopic equilibration of the Earth-Moon system after the giant impact (Pahlevan and Stevenson, 2007; Young et al., 2016), or (ii) the derivation of the proto-Earth and the impactor from the same, isotopically homogeneous reservoir of material (Jacobsen et al., 2013; Dauphas et al., 2014b). Thus, the Earth and Moon's identical Ca isotopic signatures remain a significant characteristic of the system that dynamical models need to reproduce.

Twelve Martian samples have been analyzed for non-mass-dependent Ca isotopic compositions. Five samples do not exhibit distinct non-mass-dependent 40 Ca/ 44 Ca, 43 Ca/ 44 Ca, or 46 Ca/ 44 Ca compared to Earth (Simon et al., 2009; Chen et al., 2011) (**Fig. 4**). The two exceptions, ALH84001 and QUE9420, have slightly elevated ε^{40} Ca/ 44 Ca compositions (+0.59 and +0.88, respectively). These small excesses are likely not a primary feature, but rather may be attributed to an unrecognized secondary alteration process on Mars (Simon et al., 2009). Additionally, Chen et al. (2011) and Schiller et al. (2018) measured the ε^{40} Ca/ 44 Ca compositions of nine Martian meteorites. While Chen et al. (2011) did not detect any significant departures of Martian meteorites from Earth, Schiller et al. (2018), who measured at slightly higher precision, found that they exhibit an average resolvable ε^{40} Ca/ 44 Ca deficit of -0.2 ± 0.03 compared to Earth.

More than 20 samples have been analyzed for mass-dependent Ca isotopic compositions (Fig. 5). Magna et al. (2015) performed the most comprehensive tucky by measuring the massdependent Ca isotopic composition of 22 different shergottites, nathlites, chassignites (SNCs), and a Martian OPX (ALH84001, and demonstrated that he verage δ⁴⁴Ca/⁴⁰Ca of Martian meteorites is indistinguishable from Earth, ordinary chonacites, and enstatite chondrites, within analytical uncertainty. Similarly, Simon and DePaylo (2010) did not identify δ^{44} Ca/ 40 Ca variation in a shergottite and ALH94001. Combining the Latasets from Magna et al. (2015) and Simon and DePaolo (2010), Martian meteorites e thio t a range in δ^{44} Ca/ 40 Ca of $\sim +0.4\%$ (from δ⁴⁴Ca/⁴⁰Ca +0.71 to +1.15) and may reflect pass-dependent Ca isotope fractionation during magmatic differentiation, though this has not been explored in detail. Magna et al. (2015) estimated a mean δ^{44} Ca/ 40 Ca of +1.04 ± 0.05 for bulk silicate Mars, identical to the estimate for BSE by Kang et al., (2017), which is consistent with the assertion made by Simon and DePaolo (2010) of uniform bulk Ca isotopi: a mpositions of the inner Solar System planets. The similarity in δ^{44} Ca/ 40 Ca between Max and the Earth can be interpreted to indicate that isotopic homogenization for Ca was cor plear by the time the inner Solar System planets formed (Simon et al., 2009).

As with Earth, there is a general consensus that Mars accreted from a mixture of materials represented by known meteorite types. Given that the estimated δ^{44} Ca/ 40 Ca composition of bulk silicate Mars overlaps with those of ordinary chondrites, enstatite chondrites, some carbonaceous chondrite types, and most achondrites, the constraints that mass-dependent Ca isotopic data place on the building blocks of Mars are limited. Nevertheless, a variety of models have been proposed. Most attempts to model combinations of precursor material types based on stable isotope constraints agree that the likely building blocks of Mars were predominantly non-carbonaceous (Lodders and Fegley, 1997; Sanloup et al., 1999; Mohapatra and Murty, 2003; Burbine and O'Brien, 2004; Tang and Dauphas, 2014; Fitoussi et al., 2016; Liebske and Khan, 2019). There is disagreement, however, in the relative proportions of precursor types. For example, Lodders and Fegley calculated that Mars could be made of 85% ordinary chondrites +11% CV chondrites +4% CI chondrites. In contrast, the results of the model from Sanloup et al. (1999) point to an exclusively non-carbonaceous Mars, made up of 55% H chondrites + 45% enstatite chondrites. This was subsequently confirmed by the results of Tang

and Dauphas (2014). Dauphas et al. (2014a) calculated ε^{48} Ca/ 40 Ca compositions for bulk Mars using the mixtures proposed by Lodders and Fegley (1997) and Sanloup et al. (1999) and found that only the value (-0.24 ± 0.30) produced by assuming the mixture of Sanloup et al. (1999) agreed with the average ε^{48} Ca/ 40 Ca composition (-0.11 ± 0.16) for SNCs measured by Chen et al. (2011). However, neither the Lodders and Fegley (1997) nor Sanloup et al. (1999) models, or any in the studies mentioned above, were able to self-consistently explain isotopic data, major element chemistry, and geophysical properties simultaneously.

5. Future directions

The field of Ca isotope cosmochemistry is rapidly expanding as new research pathways emerge. A promising avenue of research is to assess which (and to what extent) nebular processes fractionate Ca isotopes. This could be advanced by obtaining coupled mass-dependent and non-mass-dependent Ca isotopic data on disk condensates a dataset would identify if the thermal events that caused non-mass-dependent Ca isotope anon alies were linked to events that generated mass-dependent Ca isotope fractionation (e.g., Niederer and Papanastassiou, 1984; Huang et al., 2012; Simon et al., 2017; Bermingham et al., 2018).

Another research pathway would be investigating how Ca isotopes fractionate in response to parent body and terrestrial aqueous alteration processes. On parent bodies, multistage, low-temperature aqueous events mobilized and redistributed elements within the matrix and between individual components and the mutrix (e.g., McGuire and Hashimoto, 1989; Kojima & Tomeoka 1996; Krot et al. 2000b; McSween, 1987; Brealey, 2006). As Ca is fluid mobile, it is potentially sensitive to isotopic fractional on effects as a result of elemental redistribution among primary phases and/or the formation call accordary phases. Post-fall terrestrial weathering may also have resulted in Ca isotope flactionation, depending on the residence time and location of the meteorite (e.g., Gounelle and Zolensky, 2001; Bland et al., 2006). Presently, there exists only indirect or presumed evidence of Ca isotopic fractionation in meteorites as a result of aqueous alteration on the bulk scale (e., Magna et al., 2015; Deng et al., 2018; Bermingham et al., 2018) and on the component scale (e.g., Bermingham et al., 2018). An important research focus for the near future is to identify potential mass-dependent Ca isotopic effects of parent body and terrestrial aqueous alteration events on bulk meteorites and their components. Determining the extent to which these effects obscure primary mass-dependent Ca isotopic variability is required to identify planetary building blocks (Simon and DePaolo, 2010; Valdes et al., 2014; Simon et al., 2017; Bermingham et al., 2018).

Future studies that concurrently collect mass-dependent and non-mass-dependent Ca isotopic data in component and bulk samples will be most informative in addressing the significance of anomalous Ca isotopic compositions in chondrite components regarding mixing processes and the location of parent body reservoirs in the disk. The use of multi-isotopic proxies of elements that record thermal processing events (e.g., REE, O, Al, Mg, and Ti), along with Ca, will be particularly useful for providing constraints on the physical conditions of different parts of the protoplanetary disk (Bermingham et al., 2018). Forthcoming work should continue to take

advantage of the extensive datasets that have made Ca isotopes a benchmark for comparison with other isotope systems. This approach is required if a comprehensive, self-consistent formation model of the Solar System is to be formulated using isotopic datasets derived from meteorites and their components.

To this end, future work would benefit from refining current high-precision isotope measurement techniques for bulk rocks and components and coupling them with petrographic observations, mineral compositional data, major and trace element data, and *in situ* analytical and imaging techniques. This work could include advancing established analytical techniques (e.g., SIMS, NanoSIMS, and LA-MC-ICP-MS), or employing new ones such as atom probe tomography (APT) which are increasingly being used in geo- and cosmochemistry to determine isotopic compositions and spatial distributions in three dimensions at the nanometer level (e.g., Heck et al. 2014; Greer et al., 2020). Future studies may also consider using advanced micromilling techniques (following Simon et al., 2017) to completely remove components and their rims for *ex situ* work.

Finally, we emphasize the importance of standardizing future Ca isotopic data reporting methods. A significant problem in the Ca isotope community is that the direct comparison of published datasets is hindered by the lack of universal agreement on which reference material should be used as the standard for Ca isotopes. Con equently, over the years Ca isotopic data have been reported relative to many different reference materials (e.g., SRM915a, SRM915b, CaF₂, modern seawater, and BSE). This is for ther complicated by the fact that mass-dependent Ca isotope studies are inconsistent in which a stope ratios they report. Some report, for example, deviations in ⁴⁴Ca/⁴⁰Ca, ⁴⁰Ca/⁴⁴Ca, ⁴⁴Ca/⁴²Ca, or ⁴²Ca/⁴⁴Ca, while others report data as F_{Ca} (δ⁴⁰Ca/⁴⁴Ca or δ⁴⁴Ca/⁴⁰Ca in %/amu · r · r non-mass-dependent data, many studies are unclear about or make no mention of vnish isotope ratio and mass fractionation law are used to normalize and correct for instrumental mass bias. In order to limit unnecessary complexity in the comparison of cosmochemica. Ca isotopic datasets, we encourage more uniformity in data reporting. Specifically, we recommend the presentation of mass-dependent variations in the form of δ^{44} Ca/ 40 Ca and the conversion of data to the SRM915a scale, regardless of original reference material, to facilitate interlaboratory comparison. For non-mass-dependent data, we propose that data are normalized to the terrestrial ⁴²Ca/⁴⁴Ca composition relative to CaF₂ as defined by Russell et al. (1978) using the appropriate mass fractionation law for the study.

6. Conclusions

The chemical properties of Ca make its isotopes among the most robust tracers of cosmochemical processes. Here, mass-dependent and non-mass-dependent Ca isotopic variations among bulk meteorites and their components have been explored in the context of tracing the establishment and preservation of non-mass-dependent heterogeneities in the disk, understanding the effects of nebular thermal processing, and constraining the compositions of planetary building blocks.

Well resolved non-mass-dependent isotope effects, generally considered to be the result of a poorly homogenized protoplanetary disk, are present in both bulk chondrites and their components. It is clear from these variations that isotopically distinct contributions of various nucleosynthetic origins were incorporated into the disk and survived long enough to be preserved in planet-building materials. Debate, however, persists as to how and when the presolar grain carriers of these Ca isotope anomalies became heterogeneously distributed in the disk. Presently, non-mass-dependent Ca isotope anomalies in most chondrite components are decoupled from mass-dependent variations. This suggests the thermal processing events that generated Ca isotope anomalies occurred at a different time or location in the protoplanetary disk from those that generated mass-dependent Ca isotope fractionations.

Compared to chondrite components, bulk meteorites display limited, but resolved, mass-dependent and non-mass-dependent Ca isotope variations. In the context of chondritic Earth models, these variations provide constraints on the genetic links between chondrites and Earth, as well as between Earth and the Moon. Specifically, Ca isotopic data support the interpretation that 1) material isotopically similar to ordinary or enstant chondrites comprised a significant portion of the precursors that accreted to Earth, and 2) the Moon may have formed predominantly from proto-Earth material, or, if from in pactor material, then only if the impactor had the same isotopic composition as the proto-Earth or if the vaporous material from both fully homogenized after impact. These interpretations, nowever, rely on the assumption that bulk samples are representative of parent body cor positions. Determining the extent to which parent body and terrestrial alteration effects obscure primary mass-dependent Ca isotope variability is central to constraining the nature of plane tary building blocks.

Acknowledgements:

Authors would like to thank 'he editors for their guidance and patience. We would like to thank two anonymous reviewers for their comments. We are grateful to Andy Davis for his insightful comments which improved the manuscript, Nikolaus Gussone for assistance with δ⁴⁴Ca/⁴⁰Ca conversions Letwien different standards, and Hamed Pourkhorsandi and François Tissot for constructive accussions. M.C.V. was supported by the Fondation Wiener-Anspach Postdoctoral Fellowship at the University of Cambridge and the John Caldwell Meeker Postdoctoral Fellowship through the Negaunee Integrative Research Center's Robert A. Pritzer Center for Meteoritics and Polar Studies at the Field Museum. K.R.B. received support from NASA Emerging Worlds grants 80NSSC18K0496 and NNX16AN07G, NASA SSERVI grant NNA14AB07A, and the Department of Earth and Planetary Sciences, Rutgers University. S.H. was supported by NSF grant AST-1910955. J.I.S. was supported by NASA Planetary Science Division, Solar System Workings, and Emerging Worlds Programs.

Conflicts of interest

The authors certify that they have no conflicts of interest to declare. All co-authors have seen and agree with the contents of the manuscript and there is no financial interest to report. We certify that the submission is original work and is not under review at any other publication.

References

Akram, W., Schönbächler, M., Bisterzo, S., and Gallino, R. 2015. Zirconium isotope evidence for the heterogeneous distribution of s-process materials in the Solar System. Geochim. Cosmochim. Acta 165, 484-500.

Alexander, C. M. O'D., Grossman, J. N., Ebel, D. S., and Ciesia, F. J. 2008. The Formation conditions of chondrules and chondrites. Science 320, 1617-1617.

Allègre, C. J., Poirier, J. -P., Humler, E., and Hofmann, A. V. 1995. The chemical composition of the Earth. Earth Planet. Sci. Lett. 134, 515–526.

Allen, J. M., Grossman, L., Lee, T., and Wasserburg G. J. 1979. Mineralogical study of an isotopically-unusual Allende inclusion. Lunar Planet. Sci. 10, 24-26.

Allen, J. M., Grossman, L., Lee, T., and Wasserburg., G. J. 1980. Mineralogy and petrography of HAL, an isotopically-unusual Allende inclusion. Geochim. Cosmochim. Acta 44, 685–699.

Amari, S., Anders, E., Virag, A., and Zimar E. 1990. Interstellar graphite in meteorites. Nature 345, 238-240.

Amos, S., Gross, J. L., and Thoenne St. M. 2011. Discovery of the calcium, indium, tin, and platinum isotopes. At. Data Nucl. Data 12,bles 97, 383–402.

Amsellem, E. Moynier, F., Pringio E. A., Bouvier, A., Chen, H., and Day, J. M. D. 2017. Testing the chondrule-rich accretion model for planetary embryos using calcium isotopes. Earth Planet. Sci. Lett. 469, 75–83.

Amsellem, E, Moynier, I' and Puchtel, I S. 2019. Evolution of the Ca isotopic composition of the mantle. Geochim. Co. mochim. Acta 258, 195–206.

Anders, E. 1971. How well do we know "cosmic" abundances? Geochim. Cosmochim. Acta, 35, 516–522.

Anders, E. and Grevesse, N. 1989. Abundances of the elements: Meteoritic and Solar. Geochim. Cosmochim. Acta 53, 197-214.

Antonelli, M. A. and Simon, J. I. 2020. Calcium isotopes in high-temperature terrestrial processes. Chem. Geol. 548, 119651.

Armytage, R. M. G., Georg, R. B., Williams, H. M., and Halliday, A. N. 2012. Silicon isotopes in lunar rocks: Implications for the Moon's formation and the early history of the Earth. Geochim. Cosmochim. Acta 77, 504-514.

- Bermingham, K. R. 2011. Stable Ba and Ca isotope compositions of meteorites and their components: Insights into the early Solar System. PhD thesis, Westfälische Wilhelms-Universität. pp. 98-102.
- Bermingham, K. R., Mezger, K., Scherer, E. E., Horan, M. F., Carlson, R. W., Upadhyay, D., Magna, T., and Pack, A. 2016. Barium isotope abundances in meteorites and their implications for early Solar System evolution. Geochim. Cosmochim. Acta 175, 282-298.
- Bermingham, K. R., Gussone, N., Mezger, K., and Krause, J. 2018. Origins of mass-dependent and mass-independent Ca isotope variations in meteoritic components and meteorites. Geochim. Cosmochim. Acta 226, 206–223.
- Bernatowicz, T., Fraundorf, G., Tang, M. Anders, E., Wopenka, B, Zinner, E., and Fraundorf, P. 1987. Evidence for interstellar SiC in the Murray carbonaceous me Porite. Nature 330, 24-31.
- Binzel, R. P. 1996. Searching for resolution in the S-asteroid ordinary chondrite debate. Meteorit. Planet. Sci. 31, 165.
- Bischoff, A. and Keil, K. 1984. Al-rich objects in or inary chondrites: Related origin of carbonaceous and ordinary chondrites and their constituents. Geochim. Cosmochim. Acta 48, 693-709.
- Bischoff, A. Vogel, N. and Roszjar, J. 2011 The Rumuruti chondrite group. Chem. Erde/Geochemistry 71, 101–133.
- Black, D. C. and Pepin, R. O. 1969. Trainer neon in meteorites II. Earth Planet. Sci. Lett. 6, 395–405.
- Bland, P. A., Alard, O., Benedix, G. K., Kearsley, A. T., Menzies, O. N., Watt, L. E., and Rogers, N. W. 2005. Volatile fraction in the early Solar System and chondrule/matrix complementarity Proc. Natl. Acad Sci. 102, 13755-13760.
- Bland, P. A., Zolensky, M. E., Benedix, G. K., and Sephton, M. A. 2006. Weathering of chondritic meteorites. In: Meteorites and the early Solar System II (Eds. Lauretta, D. S. and McSween, H. Y. Jr.), University of Arizona Press, 853-867.
- Bogard, D. D., Nyquist, L. E., Bansal, B. M., Garrison, D. H., Wiesmann, H., Herzog, G. F., Albrecht, A. A., Vogt, S., and Klein, J. 1995. Neutron-capture ³⁶Cl, ⁴¹Ca, ³⁶Ar, and ¹⁵⁰Sm in large chondrites: Evidence for high fluences of thermalized neutrons. J. Geophys. Res. 100, 9401–9416.
- Bonnand, P., Parkinson, I. J., and Anand, M. 2016. Mass dependent fractionation of stable chromium isotopes in mare basalts: implications for the formation and the differentiation of the Moon. Geochim. Cosmochim. Acta 175, 208-221.
- Boss, A. P. 1995. Collapse and fragmentation of molecular cloud cores. II. Collapse induced by stellar shock waves. Astrophys. J. 439, 224–236.
- Bottke, W. F., Nesvorný, D., Grimm, R. E., Morbidelli, A., and O'Brien D. P. 2006. Iron meteorites as remnants of planetesimals formed in the terrestrial planet region. Nature 439, 821-824.

Boynton, W. V. 1975. Fractionation in the Solar nebula: condensation of yttrium and the rare earth elements. Geochim. Cosmochim. Acta 39, 569-584,

Brearley, A. J. 2006. The action of water. In: Meteorites and the early Solar System II (Eds. Lauretta, D. S. and McSween, H. Y. Jr.), University of Arizona Press, 587-624.

Brearley, A. J. and Jones, R. H. 1998. Chondritic meteorites. In: Planetary Materials (Ed. Papike, J. J.), Reviews in Mineralogy 36, Mineralogical Society of America, 3.1-3.398.

Budde, G. Burkhardt, C., and Kleine, T. 2019. Molybdenum isotopic evidence for the late accretion of outer Solar System material to Earth. Nat. Astron. 3, 736–741.

Bullock, E. S., Knight, K. B., Richter, F. M., Kita, N. T., Ushikubo, T., MacPherson, G. J., Davis, A. M., and Mendybaev, R. A. 2013. Mg and Si isotopic fractionation patterns in types B1 and B2 CAIs: Implications for formation under different nebular conditions. Meteorit. Planet. Sci. 48, 1440–1458.

Burbidge, E. M., Burbidge, G. R., Fowler, W. A., and Hoyle F. 1957. Synthesis of the elements in stars. Rev. Mod. Phys. 29, 547–650.

Burbine, T. H. and O'Brien, K. M. 2004. Determining 'he possible building blocks of the Earth and Mars. Meteorit. Planet. Sci. 39 667-68.

Cameron, A.G.W. 1957. Stellar evolution, nuclear ast ophysics, and nucleogenesis. Chalk River Report, CLR-41, Chalk River, Ontario. pp. 1-197.

Cameron, A. G. W. 2000. Higher resolutio. simulations of the Giant Impact. In: Origin of the Earth and Moon (Eds. Canup, R. M. and Righter, K.), University of Arizona Press, 133-144.

Cameron, A. G. W. 1962. The format or A f the Sun and planets. Icarus 1, 13-69.

Cameron, A. G. W. and Truran, W. 1977. The supernova trigger for formation of the Solar System. Icarus 30, 447–461.

Cameron, A. G. W. and Wai 1, W. R. 1976. The origin of the Moon. Lunar Sci. 7, 120-122.

Canup, R. M. and Aspha ig, 3. 2001. Origin of the Moon in a giant impact near the end of the Earth's formation. Nature 412, 708-712.

Canup, R. M. 2012. Forming a Moon with an Earth-like composition via a giant impact. Science. 338, 1052-1055.

Chambers, J. E. 2001. Making more terrestrial planets. Icarus 152, 205–224.

Chen, H. -W., Lee, T., Lee, D. -C., Shen, J. J. -S., and Chen, J. -C. 2011. ⁴⁸Ca heterogeneity in differentiated meteorites. Astrophys. J. 743, L23.

Chen, H. -W., Lee, T., Lee, D. -C., and Chen, J. -C. 2015. Correlation of ⁴⁸Ca, ⁵⁰Ti, and ¹³⁸La heterogeneity in the Allende refractory inclusions. Astrophys. J.806, L21.

Clayton, R. N. 2002. Self-shielding in the Solar nebula. Nature 415, 860–861.

- Clayton, R. N. 2004. Oxygen isotopes in meteorites. In: Meteorites, Planets, and Comets (Ed. Davis, A. M.), Vol. 1 Treatise on Geochemistry (Eds. Holland, H. D. and Turekian, K. K.), Elsevier, Oxford, 129–142.
- Clayton, R. N., Grossman, L., and Mayeda, T. K. 1973. A component of primitive nuclear composition in carbonaceous meteorites. Science 182, 485–488.
- Connelly, J. N., Bizzarro, M., Krot, A.N., Nordlund, Å., Wielandt, D., and Ivanova, M.A. 2012. The absolute chronology and thermal processing of solids in the Solar protoplanetary disk. Science 338, 651.
- Craddock, P.R. and Dauphas, N. 2011. Iron isotopic compositions of geological reference materials and chondrites. Geostand. Geoanal. Res. 35, 101-123.
- Ćuk, M. and Stewart, S. T. 2012. Making the Moon from a fast-spin ping Earth: A giant impact followed by resonant despinning. Science 338, 1047-1052.
- Cuzzi, J. N. and Alexander, C. M. O. 2006. Chondrule formation in particle- rich nebular regions at least hundreds of kilometres across. Nature 441, 483–48.
- Dauphas, N., Remusat, L., Chen, J. H., Roskosz, M., Forar astassiou, D. A., Stodolna, J., Guan, Y., Ma, C., and Eiler, J. M. 2010. Neutron-rich chomom isotope anomalies in supernova nanoparticles. Astrophys. J. 720, 1577-1591.
- Dauphas, N., Chen, J. H., Zhang, J., Papanastarsiou, D. A., Davis, A. M., and Travaglio, C. 2014a. Calcium-48 isotopic anomalies in halk chondrites and achondrites: Evidence for a uniform isotopic reservoir in the inner protopic netary disk. Earth Planet. Sci. Lett. 407, 96–108.
- Dauphas, N., Burkhardt, C., Warren, F. H. and Teng, F. -Z. 2014b. Geochemical arguments for an Earth-like Moon-forming impactor. Thuos. Trans. R. Soc. A 372, 20130244.
- Dauphas, N. 2017. The isotopic nature of the Earth's accreting material through time. Nature 541, 521–524.
- Davis, A. M. and Grossman, Y. 1979. Condensation and fractionation of rare earths in the Solar nebula. Geochim. Cosmo hin . Acta 43, 1611-1632.
- Davis, A. M., Tanaka, A., Grossman, L., Lee, T., and Wasserburg, G. J., 1982. Chemical composition of HAL, an isotopically-unusual Allende inclusion. Geochim. Cosmochim. Acta 46, 1627-1651.
- Davis, A. M., Hashimoto, A., Clayton, R. N., and Mayeda, T. K. 1990. Isotope mass fractionation during evaporation of Mg₂SiO₄. Nature 347, 655–658.
- Davis, A. M., Richter, F. M., Mendybaev, R. A., Janney, P. E., Wadhwa, M., and McKeegan, K. D. 2015. Isotopic mass fractionation laws for magnesium and their effects on ²⁶Al–²⁶Mg systematics in Solar system materials. Geochim. Cosmochim. Acta 158, 245–261.
- Davis, A. M., Zhang, J., Greber, N. D., Hu, J., Tissot, F. L. H., and Dauphas, N. 2018. Titanium isotopes and rare earth patterns in CAIs: evidence for thermal processing and gas-dust decoupling in the protoplanetary disk. Geochim. Cosmochim. Acta 221, 275-295.

- Deng, Z., Moynier, F, van Zuilen, K., Sossi, P. A., Pringle, E. A., and Chaussidon, M. 2018. Lack of resolvable titanium stable isotopic variations in bulk chondrites. Geochim. Cosmochim. Acta 239, 409-419.
- Drake, M. J. and Righter, K. 2002. Determining the composition of the Earth. Nature 416, 39-44.
- Esat, T. M., Spear, R. H., and Taylor., S. R. 1986. Isotope anomalies induced in laboratory distillation. Nature 319, 576–578.
- Fahey, A., Goswami, J. N., McKeegan, K. D., and Zinner, E. 1987a. ²⁶Al, ²⁴⁴Pu, ⁵⁰Ti, REE, and trace element abundances in hibonite grains from CM and CV meteorites. Geochim. Cosmochim. Acta 51, 329-350.
- Fahey, A. J., Goswami, J. N., McKeegan, K. D., and Zinne E. 1987b. ¹⁶O excesses in Murchison and Murray hibonites: A case against a late supernova injection origin of isotopic anomalies in O, Mg, Ca, and Ti. Astrophys. J. 323, L91-L95.
- Fantle, M. S. and Tipper, E. T. 2014. Calcium isotopes in the global biogeochemical Calcycle: implications for development of a Calisotope proxy. Earth Voi. Kev. 129, 148–177.
- Fischer-Gödde, M., Burkhardt, C., Kruijer, T. S., and Teire, T. 2015. Ru isotope heterogeneity in the Solar protoplanetary disk. Geochim. Cosmochim. Aca 168, 151-171.
- Fitoussi, C., Bourdon, B., Pahlevan, K. and Wie'e. R 2010. Si isotope constraints on the moon-forming impact. Lunar Planet. Sci. 41, #1532.
- Fitoussi, C., Bourdon, B., and Wang, X. 2016. The building blocks of Earth and Mars: A close genetic link. Earth Planet. Sci. Lett. 435, 151-160.
- Galy, A. Young, E. D., Ash, R. D., and O'Nions, R. K. 2000. The formation of chondrules at high gas pressures in the Solar nebule collected 290, 1751–1754.
- Goswami, J. N. 2004. Short-lived nuclides in the early Solar System: the stellar connection. New Astron. Rev. 48, 125–132.
- Gounelle, M. and Zolens', M. E. 2001. A terrestrial origin for sulfate veins in CI1 chondrites. Meteorit. Planet. Sci. 35, 132,-1329.
- Gradie, J. C. and Tedesco, E. F. 1982. Compositional structure of the asteroid belt. Science 216, 1405–1407.
- Greer, J. Rout, S. S., Isheim, D., Seidman, D. N, Wieler, R., and Heck, P. R. 2020. Atom probe tomography of space-weathered lunar ilmenite grain surfaces. Meteorit. Planet. Sci. 55, 426-440.
- Grewal, D. S., Dasgupta, R., Sun, C., Tsuno, K., and Costin, G. 2019. Delivery of carbon, nitrogen, and sulfur to the silicate Earth by a giant impact. Sci. Adv. 5, 1-12.
- Grimm, R. E. and McSween, H. Y. Jr. 1993. Heliocentric zoning of the asteroid belt by aluminum-26 heating. Science 259, 653–655.
- Grossman, L. 1972. Condensation in the primitive Solar nebula. Geochim. Cosmochim. Acta 36, 597–619.

- Grossman, L. and Steele, I. 1976. Amoeboid olivine aggregates in the Allende meteorite. Geochim. Cosmochim. Acta 40, 149-155.
- Grossman, L., Ebel, D. S., Simon, S. B., Davis, A. M., Richter, F. M., and Parsad, N. M. 2000. Major element chemical and isotopic compositions of refractory inclusions in C3 chondrites: the separate roles of condensation and evaporation. Geochim. Cosmochim. Act, 64, 2879–2894.
- Hartmann, W.K. and Davis, D.R. 1975. Satellite-sized planetesimals and lunar origin. Icarus 24, 504-514.
- He, Y., Wang, Y., Zhu, C., Huang, S. and Li, S. 2017. Mass-independent and mass dependent Ca isotopic compositions of thirteen geological standards measured by thermal ionization mass spectrometry. Geostand. Geoanal. Res. 41, 283-302.
- Heck, P. R., Stadermann, F. J., Isheim, D., Auciello, O., Daulton, T. L., Davis, A. M., Elam, J. W., Floss, C., Hiller, J., Larson, D. J., Lewis, J. B., Mane, A., Pellin, M. J., Savina, M. R., Seidman, D. N., and Stephan, T. 2014. Atom-probe analyses of nanodiamonds from Allende. Meteorit. Planet. Sci. 49, 453-467.
- Heck, P. R., Greer, J., Kööp, L., Trappitsch, R., Gyngar 1, 1, Busemann, H., Maden, C., Ávila, J. N., Davis, A. M., and Wieler, R. 2020. Lifetimes of incordellar dust from cosmic ray exposure ages of presolar silicon carbide. Proc. Natl. Acad. Sci. 1107, 1884–1889.
- Heuser, A., Eisenhauer, A., Gussone, N., Bork, C., Hansen, B. T., and Nägler, T. F. 2002. Measurement of calcium isotopes (δ^{44} Ca) using a multicollector TIMS technique. Int. J. Mass Spectrom. 220, 387–399.
- Hinton, R. W. and Bischoff, A. 1984. Io. microprobe magnesium isotope analysis of plagioclase and hibonite from ordinary chondrites. No ture 308, 169-172.
- Hinton, R. W., Davis, A. M., Screen, -Wachel, D. E., Grossman, L., and Draus, R. J. 1988. A chemical and isotopic study of n. bonite-rich refractory inclusions in primitive meteorites. Geochim. Cosmochim. Acta 52 2573–2598.
- Hippler, D., Schmitt, A.P., Gussone, N., Heuser, A., Stille, P., Eisenhauer, A., and Nägler, T.F. 2003. Calcium isotopic composition of various reference materials and seawater. Geostand. Newsl. 27, 13-19
- Hopp, T. Budde, G., and Kleine, T. 2020. Heterogeneous accretion of Earth inferred from Mo-Ru isotope systematics. Earth Planet. Sci. Lett. 534, #116065 (17 pp).
- Huang, F., Zhou, C., Wang, W., Kang, J., and Wu, Z. 2019. First-principles calculations of equilibrium Ca isotope fractionation: Implications for oldhamite formation and evolution of lunar magma ocean. Earth Planet. Sci. Lett. 510, 153-160.
- Huang, S. and Jacobsen, S. B. 2017. Calcium isotopic compositions of chondrites. Geochim. Cosmochim. Acta 201, 364–376.
- Huang, S. Farkas, J., and Jacobsen, S. B. 2010. Calcium isotopic fractionation between clinopyroxene and orthopyroxene from mantle peridotites. Earth Planet. Sci. Lett. 292, 337–344.

- Huang, S., Farkas, J., Yu, G., Petaev, M. I., and Jacobsen, S. B. 2012. Calcium isotopic ratios and rare earth element abundances in refractory inclusions from the Allende CV3 chondrite. Geochim. Cosmochim. Acta 77, 252–265.
- Humayun, M. and Cassen, P. 2000. Processes determining the volatile abundances of the meteorites and terrestrial planets. In: Origin of the Earth and Moon (Eds. Canup, R. M. and Righter, K.), University of Arizona Press, 3-24.
- Ireland, T. R. 1988. Correlated morphological, chemical, and isotopic characteristics of hibonites from the Murchison carbonaceous chondrite. Geochim. Cosmochim. Acta 52, 2827–2839.
- Ireland, T. R. 1990. PreSolar isotopic and chemical signatures in hibonite-bearing refractory inclusions from the Murchison carbonaceous chondrite. Geochim Cosmochim. Acta 54, 3219–3237.
- Ireland, T. R. and Compston, W. 1987. Large heterogeneous ² Mg excesses in a hibonite from the Murchison meteorite. Nature 327, 689-692.
- Ireland, T. R., Fahey, A. J., and Zinner, E. K. 1989. Isolvoic and chemical constraints on the formation of HAL-type refractory inclusions. Lunar Pla iet. Sci. 20, 442-443.
- Ireland, T. R., Fahey, A. J., and Zinner, E. K. 1991. Hit nite-bearing microspherules: A new type of refractory inclusions with large isotopic arc malies. Geochim. Cosmochim. Acta 55, 367–379.
- Ireland, T. R., Zinner, E. K., Fahey, A. J., and Esat, T. M. 1992. Evidence for distillation in the formation of HAL and related hibonite inclusions. Geochim. Cosmochimi. Acta 56, 2503–2520.
- Jacobsen, B., Yin, Q. -Z., Moynier, F. Anclin, Y., Krot, A. N., Nagashima, K., Hutcheon, I. D., and Palme, H. 2008. ²⁶Al-²⁶Mg and ²⁰ Po-²⁰⁶Pb systematics of Allende CAIs: canonical Solar initial ²⁶Al/²⁷Al ratio reinstated. Earth Planet. Sci. Lett. 272, 353-364.
- Jacobsen, S. B., Petaev, M., Huang, S. and Sasselov, D. 2013. An isotopically homogeneous inner terrestrial planet region. Mineral. Mag. 77, 1371.
- Johansen, A. and Lambrechts M. 2017. Forming planets via pebble accretion. Annu. Rev. Earth Planet. Sci. 45, 359–387.
- Javoy, M. 1995. The integral enstatite chondrite model of the Earth. Geophys. Res. Lett. 22, 2219–2222.
- Javoy, M. and Pineau, F. 1983. Stable isotope constraints on a model Earth, from a study of mantle nitrogen. Meteoritics 18, 320-321.
- Javoy, M., Kaminski, E., Guyot, F., Andrault, D., Sanloup, C., Moreira, M., Labrosse, S., Jambon, A., Agrinier, P., and Davaille, A. 2010. The chemical composition of the Earth: Enstatite chondrite models. Earth Planet. Sci. Lett. 293, 259–268.
- Jordan, M. K., Young, E. D., and Jacobsen, S. B. 2013. Mg and Si isotope fractionation in Allende CAI SJ101 as a result of condensation. Lunar Planet. Sci. 44, #3052.
- Jungck, M. H. A., Shimamura, T., and Lugmair, G. W. 1984. Ca isotope variation in Allende. Geochim. Cosmochim. Acta 48, 2651–2658.

- Kang, J. T., Zhu, H. L., Liu, Y. F., Liu, F., Wu, F., Hao, Y. T., Zhi, X. C., Zhang, Z. F., and Huang, F. 2016. Calcium isotopic composition of mantle xenoliths and minerals from Eastern China. Geochim. Cosmochim. Acta 174, 335–344.
- Kargel, J. S. and Lewis, J. S. 1993. The composition and early evolution of Earth. Icarus 105, 1–25.
- Kleine, T., Mezger, K., Palme, H., Scherer, E., and Münker, C., 2005. Early core formation in asteroids and late accretion of chondrite parent bodies: evidence from ¹⁸²Hf⁻¹⁸²W in CAIs, metalrich chondrites, and iron meteorites. Geochim. Cosmochim. Acta 69, 5805–5818.
- Knight, K. B., Kita, N. T., Mendybaev, R. A., Richter, F. M., Davis, A. M., and Valley, J. W. 2009. Silicon isotopic fractionation of CAI- like vacuum evaporation residues. Geochim. Cosmochim. Acta 73, 6390–6401.
- Kojima, T. and Tomeoka, K. 1996. Indicators of aqueous alteration and thermal metamorphism on the CV parent body: Microtextures of a dark inclusion from Anende. Geochim. Cosmochim. Acta 60, 2651-2666.
- Kööp, L., Davis, A. M., Nakashima, D., Park, C., Krot, A. N., Nagashima, K., Tenner, T. J., Heck, P. R., and Kita, N. T. 2016a. A link between oxygen, calcium and titanium isotopes in ²⁶Al-poor hibonite-rich CAIs from Murchison and implications for the heterogeneity of dust reservoirs in the Solar nebula. Geochim. Cosmoch v.i. Acta 189, 70–95.
- Kööp, L., Nakashima, D., Heck, P. R., Kila, N. T., Tenner, T. J., Krot, A. N., Nagashima, K., Park, C., and Davis, A. M. 2016b. New contraints on the relationship between ²⁶Al and oxygen, calcium, and titanium isotopic variation in the early Solar System from a multielement isotopic study of spinel-hibonite inclusions. Geochim. Cosmochim. Acta 184, 151–172.
- Kööp, L., Davis, A. M., Krot, A. N., Nagashima, K., and Simon, S. B. 2018a. Calcium and titanium isotopes in refractory inclusions from CM, CO, and CR chondrites. Earth Planet. Sci. Lett. 489, 179–190.
- Kööp, L., Nakashima, D., Hock P. R., Kita, N. T., Tenner, T. J., Krot, A. N., Nagashima, K., Park, C., and Davis, A. M. 2018b. A multielement isotopic study of refractory FUN and CAIs: Mass-dependent and mass independent isotope effects. Geochim. Cosmochim. Acta 221, 296–317.
- Krot, A. N., Meibom, A., and Keil, K. 2000a. A clast of Bali-like oxidized CV material in the reduced CV chondrite breccia Vigarano. Meteorit Planet. Sci. 35, 817–825.
- Krot, A. N., Petaev, M. I., Meibom, A., and Keil, K. 2000b. In situ growth of Ca-rich rims around Allende dark inclusions. Geochim. Int. 38, S351-S368.
- Krot A. N., Makide K., Nagashima K., Huss G. R., Ogliore, R. C., Ciesla, F. J., Yang, L., Hellebrand, E., and Gaidos, E. 2012. Heterogeneous distribution of ²⁶Al at the birth of the Solar System: Evidence from refractory grains and inclusions. Meteorit. Planet. Sci. 47, 1948–1979.
- Krot, A. N., Keil, K., Scott, E. R. D., Goodrich, C. A., and Weisberg, M. K. 2014. Classification of meteorites and their genetic relationships. In: Meteorites and Cosmochemical Processes (Ed. Davis, A. M.), Vol. 1 Treatise on Geochemistry, 2nd Ed. (Exec. Eds. Holland, H. D., and Turekian, K. K.), Elsevier, Oxford, 1–63.

- Kruijer, T. S., Touboul, M., Fischer-Godde, M., Bermingham, K, R., Walker, R. J., and Kleine, T. 2014. Protracted core formation and rapid accretion of protoplanets. Science 344, 1150–1154.
- Kurat, G., Palme, H., Brandstatter, F., and Huth, J. 1989. Allende xenolith AF: Undisturbed record of condensation and aggregation of matter in the Solar nebula. Z. Naturforsch. A 10, 988–1004.
- Lambrechts, M. and Johansen A. 2012. Rapid growth of gas-giant cores by pebble accretion. Astron. Astrophys. 544, #A32.
- Larimer, J. W. 1971. Composition of the Earth: Chondritic or achondritic? Geochim. Cosmochim. Acta 35, 769–786.
- Larsen, K. K., Trinquier, A., Paton, C., Schiller, M., Wielandt, D. Ivanova, M. A., Connelly, J. N., Nordlund, Å., Krot, A. N., and Bizzarro, M. 2011. Evidence for magnesium isotope heterogeneity in the Solar protoplanetary disk. Astrophys. J. 735 L3 '-L47.
- Lee, T. Papanastassiou, D. A., and Wasserburg, G. J. 1978 Ca cium isotopic anomalies in the Allende Meteorite. Astrophys. J. 220, L21-L25.
- Lee, T., Russell, W. A., and Wasserburg, G. J. 1979. C. lcit m isotopic anomalies and the lack of aluminum-26 in an unusual Allende inclusion. Astrophys. J. 228, L93–L98.
- Lee, T., Mayeda, T. K., and Clayton, R. N. 1°80. Oxygen isotopic anomalies in Allende inclusion HAL. Geophys. Res. Lett. 7, 493-425.
- Lewis, R.S., Srinivasan, B., and Anders, E. 975. Host phase of a strange xenon component in Allende. Science, 190 1251-1262.
- Lewis, R. S., Tang, M., Wacker, J. J., Anders, E., and Steel, E. 1987. Interstellar diamonds in meteorites. Nature 326, 160-162.
- Liebske, C. and Khan, A. 2019. On the principal building blocks of Mars and Earth. Icarus 322, 121-134.
- Liu, M. -C. 2017. The in ua. Ca/40Ca ratios in two type A Ca-Al-rich inclusions: Implications fort he origin of short-Tve. 141Ca.
- Liu, M. -C., McKeegar, K., Goswami, J. N., Marhas, K. K., Sahijpal, S., Ireland, T. R., and Davis, A. M. 2009. Isotopic records in CM hibonites: Implications for timescales of mixing of isotope reservoirs in the Solar nebula. Geochim. Cosmochim. Acta 73, 5051-5079.
- Liu, M. -C., Chaussidon, M., Srinivasan, G., and McKeegan, K. 2012. A lower initial abundance of short-lived ⁴¹Ca in the early Solar System and its implications for Solar System formation. Astrophys. J. 761: 137.
- Liu, M. -C., Han, J., Brearley, A. J., and Hertwig, A. T. 2019. Aluminum-26 chronology of dust coagulation and early Solar System evolution. Sci, Adv. 5, eaaw3350.
- Lock, S. J., Stewart, S. T., Petaev, M. I., Leinhardt, Z., Mace, M. T., Jacobsen, S. B., and Ćuk, M. 2018. The origin of the Moon with a terrestrial synestia. J. Geophys. Res.: Planets 123, 910-951.

Lock S. J., Bermingham K. R., Parai R. and Boyet M. (2020) Geochemical constraints on the origin of the Moon and preservation of ancient terrestrial heterogeneities. Space Sci. Rev. 216, 109.

Lodders, K. 2003. Solar system abundances and condensation temperatures of the elements. Astrophys. J. 591, 1220–1247.

Lodders, K. 2020. Solar Elemental Abundances, in The Oxford Research Encyclopedia of Planetary Science, Oxford University Press.

Lodders, K. and Fegley, B. 1997. An oxygen isotope model for the composition of Mars. Icarus 126, 373-394.

Lodders, K. and Amari, S. 2005, Grains from meteorites: Remna vs from the early times of the Solar System. Chem. Erde 65, 93-166.

Lugmair, G.W. and Shukolyukov, A. 1998. Early Solar System timescales according to ⁵³Mn⁵³Cr systematics. Geochim. Cosmochim. Acta 62, 2863–2880

Lundberg, L.L., Zinner, E., and Crozaz, G. 1994. Search for isotopic anomalies in oldhamite (CaS) from unequilibrated (E3) enstatite chondrites. Me for t. Planet. Sci. 29, 384–393

Magna, T., Gussone, N., and Mezger, K. 2015. The calcium isotope systematics of Mars. Earth Planet. Sci. Lett. 430, 86-94.

MacPherson, G. J. 2014. Calcium-alum non-rich inclusions in chondritic meteorites. In: Meteorites and Cosmochemical Processes (74. Davis, A. M.), Vol. 1 Treatise on Geochemistry, 2nd Ed. (Exec. Eds. Holland, H. D. and Turekian, K. K.), Elsevier, Oxford, 139–179.

MacPherson, G. J., Bar-Matthews, M., Taka, T., Olsen, E. and Grossman, L. 1983. Refractory inclusions in the Murchison meteoric Cochim. Cosmochim. Acta 47, 823-839.

MacPherson, G. J., Davis, A. N., and Zinner, E. 1995. The distribution of aluminum-26 in the early Solar System – a reapprancal. Meteoritics 30, 365-368.

MacPherson, G. J., Kita N. 1., Ushikubo, T., Bullock, E. S., and Davis, A. M. 2012. Well-resolved variations in the formation ages for Ca–Al-rich inclusions in the early Solar System. Earth Planet. Sci. Lett. 33: -332, 43-54.

MacPherson, G. J., Simon, S. B., Davis, A. M., Grossman, L., and Krot, A. N. 2005. Calcium-aluminum-rich inclusions: Major unanswered questions. In: A. N. Krot, E. R. D. Scott, & B. Reipurth (eds.), Chondrites and the protoplanetary disk, Astronomical Society of the Pacific Conference Series (Vol. 341).

Martin, P. M. and Mason, B. 1974. Major and trace elements in the Allende meteorite. Nature 249, 333-334.

Mason, B. and Taylor, S. R. 1982. Inclusions in the Allende meteorite. Smithson. Contrib. Earth Sci. 25, 1–30.

McDonough, W. F. and Sun, S. -S. 1995. The composition of the Earth. Chem. Geol. 120, 223-253.

McGuire, A. V. and Hashimoto, A. 1989. Origin of zoned fine-grained inclusions in the Allende meteorite. Geochim. Cosmochim. Acta 53, 1123-1133.

McSween, H. Y., Jr. 1987. Aqueous alteration in carbonaceous chondrites: Mass balance constraints on matrix mineralogy. Geochim. Cosmochim. Acta 51, 2469-2477.

Meyer, B. S., Krishnan, T. D., and Clayton, D. D. 1996. ⁴⁸Ca production in matter expanding from high temperature and density. Astrophys. J. 462, 825.

Mendybaev, R.A., Beckett, J.R., Grossman, L., Stolper, E., Cooper, R.F., and Bradley, J.P. 2002. Volatilization kinetics of silicon carbide in reducing gases: an experimental study with applications to the survival of presolar grains in the Solar nebula. Geochim. Cosmochim. Acta 66, 661-682.

Mittlefehldt, D. W. 2014. Achondrites. In: Meteorites and Cosmochemical Processes (Ed. Davis, A. M.), Vol. 1 Treatise on Geochemistry, 2nd Ed. (Exec. Eds. Holland, H. D. and Turekian, K. K.), Elsevier, Oxford, 235–266.

Mohapatra, R.K. and Murty, S.V.S. 2003. Precursors of Mars: Constraints from nitrogen and oxygen isotopic compositions of Martian meteorites. Matter it. Planet. Sci. 38, 225–241.

Montmerle, T., Augereau, J.-C., Chaussidon, M., Gouneile, M., Marty B., and Morbidelli, A. 2006. Solar system formation and early evolution The first 100 million years. Earth, Moon, and Planets 98, 39-95.

Mougel, B., Moynier, F., and Gopel. C. 2017. Chromium isotopic homogeneity between the Moon, the Earth, and enstatite chondrites. Earth Planet. Sci. Lett. 481, 1-8.

Moynier, F., Simon, J. I., Podosek, F. I., Moyer, B. S., Brannon, J., and DePaolo, D. J. 2010a. Ca isotope effects in Orgueil leachates and the implications for the carrier phases of ⁵⁴Cr anomalies. Astrophys. J. 718, L7–L13.

Moynier, F., Day, J. M. D., Oku, W., Yokoyama, T., Bouvier, A., Walker, R. J., and Podosek, F. A. 2012. Planetary-scale stront im isotopic heterogeneity and the age of volatile depletion of early Solar System materials. Astrophys. J. 758, 45.

Nagahara, H. and Ozaw K. 2000. The role of back reaction on chemical fractionation during evaporation of a condense I phase. Lunar Planet. Sci. 31, #1340.

Niederer, F. R. and Papanastassiou, D. A. 1979. Ca isotopes in Allende and Leoville inclusions. Lunar Planet. Sci. 10, 913–915.

Niederer, F. R. and Papanastassiou, D. A. 1984. Ca isotopes in refractory inclusions. Geochim. Cosmochim. Acta 48, 1279–1293.

Nishiizumi, K., Fink, D., Klein, J., Middleton, R., Masarik, J., Reedy, R. C., and Arnold, J. R. 1997. Depth profile of ⁴¹Ca in an Apollo 15 drill core and the low-energy neutron flux in the Moon. Earth Planet. Sci. Lett. 148, 545–552.

Nittler, L. R., McCoy, T. J., Clark, P. E., Murphy, M. E., Trombka, J. I., and Jarosewich, E. 2004. Bulk element compositions of meteorites: A guide for interpreting remote-sensing geochemical measurements of planets and asteroids. Antarctic Meteorite Research 17, 231.

- O'Brien, D. P., Morbidelli, A., and Levison, H. F. 2006. Terrestrial planet formation with strong dynamical friction. Icarus 18, 39–58.
- Pahlevan, K. and Stevenson, D. J. 2007. Equilibration in the aftermath of the lunar-forming giant impact. Earth Planet. Sci. Lett. 262, 438-449.
- Palme, H. and O'Neill, H. 2014. Cosmochemical estimates of mantle composition. In: The Mantle and Core (Ed. Carlson, R. W.), Vol. 3 Treatise on Geochemistry, 2nd Ed. (Exec. Eds. Holland, H. D. and Turekian, K. K.), Elsevier, Oxford, 1–39.
- Palme, H., Lodders, K., and Jones, A. 2014. Solar System abundances of the elements. In: Planets, Asteroids, Comets, and the Solar System (Ed. Davis, A. M.), Vol. 2 Treatise on Geochemistry, 2nd Ed. (Exec. Eds. Holland, H. D. and Turekian K. K.), Elsevier, Oxford, 15–36.
- Pape, J., Mezger, K., Bouvier, A., and Baumgartner, L. P. 2019. Tin e and duration of chondrule formation: Constraints from ²⁶Al-²⁶Mg ages of individual ancharules. Geochim. Cosmochim. Acta 244, 416-436.
- Park, C., Nagashima, K., Wasserburg, G. J., Papanastassicu, D. A., Hutcheon, I. D., Davis, A. M., Huss, G. R., Bizzarro, M., and Krot, A. N. 2014. Calcium and titanium isotopic compositions of FUN CAIs: Implications for their origin. Lunar Planet. Sci 45, #2656.
- Park, C., Nagashima, K., Krot, A. N., Huss, G. R., Davis, A. M., and Bizzarro, M. 2017. Calcium-aluminum-rich inclusions with faction and unidentified nuclear effects (FUN CAIs): II. Heterogeneities of magnesium isotope and ²⁶Al in the early Solar System inferred from in situ high-precision magnesium isotope measurements. Geochim. Cosmochim. Acta 201, 6–24.
- Petaev, M. I. and Wood, J. A. 1900 The condensation with partial isolation (CWPI) model of condensation in the Solar nebula Teteorit. Planet. Sci. 33, 1123-1137.
- Petaev, M. I. and Jacobsen, S. B. 2009. Petrologic study of SJ101, a new forsterite-bearing CAI from the Allende CV3 chona. ite Geochim. Cosmochim. Acta 73, 5100-5114.
- Poitrasson, F., Hallid, v. A. V., Lee, D. -C., Levasseur, S., and Teutsch, N. 2004. Fe isotope differences between Earl., Moon, Mars and Vesta as possible records of contrasted accretion mechanisms. Earth Planci. Sci. Lett. 223, 253-266.
- Qin, L. and Carlson, R. W. 2016. Nucleosynthetic isotope anomalies and their cosmochemical significance. Geochem. J. 50, 43–65.
- Qin, L., Alexander, C. M. O., Carlson, R. W., Horan, M. F., and Yokoyama, T. 2010. Contributors to chromium isotope variation of meteorites. Geochim. Cosmochim. Acta 74, 1122-1145.
- Raymond, S. N., O'Brien, D. P., Morbidelli, A., and Kaib, N. A. 2009. Building the terrestrial planets: Constrained accretion in the inner Solar System. Icarus 203, 644–662.
- Regelous, M., Elliott, T., and Coath, C. D. 2008. Nickel isotope heterogeneity in the early Solar System. Earth Planet. Sci. Lett. 272, 330-338.

- Reynolds, J. H. and Turner, G. 1964. Rare gases in the chondrite Renazzo. J. Geophys. Res. 69, 3263–3281.
- Richter, F. M., Davis, A. M., Ebel, D. S., and Hashimoto, A. 2002. Elemental and isotopic fractionation of Type B calcium-, aluminum-rich inclusions: Experiments, theoretical considerations, and constraints on their thermal evolution. Geochim. Cosmochim. Acta 66, 521–540.
- Richter, F. M., Janney, P. E., Mendybaev, R. A., Davis, A. M., and Wadhwa, M. 2007. Elemental and isotopic fractionation of Type B CAI-like liquids by evaporation. Geochim. Cosmochim. Acta 71, 5544–5564.
- Rubie, D. C., Jacobson, S. A., Morbidelli, A., O'Brien, D. P., Young, E. D., de Vries, J., Nimmo, F., Palme, H. and Frost, D. J. 2015. Accretion and differentiation of the terrestrial planets with implications for the compositions of early-formed Solar System. Under and accretion of water. Icarus 248, 89-108.
- Rubin, A. E. and Wasson, J. T. 1995. Variations of character properties with heliocentric distance. Meteoritics 30, 569.
- Russell, W. A., Papanastassiou, D. A., Tombrello, T. A. 1978. Calcium isotope fractionation on the Earth and other Solar System materials. Geochim Cosmochim. Acta, 42, 1075-1090.
- Russell, S. S., Huss, G. R., Fahey, A. J., Greenvood, K. C., Hutchison, R., and Wasserburg, G. J. 1998. An isotopic and petrologic study of colleium-aluminum-rich inclusions from CO3 meteorites. Geochim. Cosmochim. Acta 62, 69–714.
- Ruzicka, A., Floss, C. and Hutson, M. 2012. Amoeboid olivine aggregates (AOAs) in the Efremovka, Leoville and Vigarano (2) 2) chondrites: A record of condensate evolution in the Solar nebula. Geochim. Cosmochim A 11, 79, 79–105.
- Sahijpal, S., Goswami, J. N., Davis, A. M., Grossman, L., and Lewis, R. S. 1998. A stellar origin for the short-lived nuclides in the early Solar System. Nature 391, 559–561.
- Sahijpal, S., Goswami, J. N. and Davis. A. M. 2000. K, Mg, Ti and Ca isotopic compositions and refractory trace element abundances in hibonites from CM and CV meteorites: Implications for early Solar System processes. Geochim. Cosmochim. Acta 64, 1989–2005.
- Sanloup, C., Jambon, A., and Gillet, P. 1999. A simple chondritic model of Mars. Phys. Earth Planet. Inter. 112, 43-54.
- Savage, P. S., and Moynier, F., 2013. Si isotopic variations in enstatite meteorites: Clues to their origin. Earth Planet. Sci. Lett. 361, 487–496.
- Schiller, M., Paton, C., and Bizzarro, M. 2015. Evidence for nucleosynthetic enrichment of the protoSolar molecular cloud core by multiple supernova events. Geochim. Cosmochim. Acta 149, 88-102.
- Schiller, M, Bizzarro, M., and Fernandes, V. A. 2018. Isotopic evolution of the protoplanetary disk and the building blocks of Earth and the Moon. Nature 555, 507–510.

- Schönbächler, M., Carlson, R. W., Horan, M. F., Mock, T. D., and Hauri, E. H. 2010. Heterogeneous accretion and the moderately volatile element budget of Earth. Science 328, 884-887.
- Scott, E. R. D. and Krot, A. N. 2014. Chondrites and their components. In: Meteorites and Cosmochemical Processes (Ed. Davis, A. M.), Vol. 1 Treatise on Geochemistry, 2nd Ed. (Exec. Eds. Holland, H. D. and Turekian, K. K.), Elsevier, Oxford, 65–137.
- Sedaghatpour, F., Teng, F. -Z., Liu, Y., Sears, D. W. G., and Taylor, L. A. 2013. Magnesium isotopic composition of the Moon. Geochim. Cosmochim. Acta 120, 1-16.
- Shahar, A. and Young, E. D. 2007. Astrophysics of CAI formation as revealed by silicon isotope LA-MC-ICPMS of an igneous CAI. Earth Planet. Sci. Lett. 257, 407–510.
- Shu, F. H., Adams, F. C., and Lizano, S. 1987. Star formation in molecular clouds: Observation and theory. Annu. Rev. Astron. Astrophys. 25, 23–72.
- Simon, J. I., Ross, D. K., Nguyen, A. N., Simon, S. B., and Ness nger, S. 2019. Molecular cloud origin for oxygen isotopic heterogeneity recorded by a primordial spinel-rich refractory inclusion. Astrophys. J. Lett. 884, #L29 (9 pp).
- Simon, J. I., Jordan, M. K., Tappa, M. J., Schauble, F. A., Kohl, I. E., and Young, E. D. 2017. Calcium and titanium isotope fractionation in refractory inclusions: Tracers of condensation and inheritance in the early Solar protoplanetary dis¹. E., in Planet. Sci. Lett. 472, 277–288.
- Simon, J. I. and DePaolo, D. J. 2010. Sably calcium isotopic composition of meteorites and rocky planets. Earth Planet. Sci. Lett. 289, 457-466.
- Simon, J. I. and Young, E. D. 2011. Resetting, errorchrons and the meaning of canonical CAI initial ²⁶Al/²⁷Al values. Earth Planet. 301. Lett. 304, 468–482.
- Simon, J. I., Young, E. D., Russel, S. S., Tonui, E. K., Dyl, K. A. and Manning, C. E. 2005. A short timescale for changing oxygen fugacity in the Solar nebula revealed by high-resolution ²⁶Al- ²⁶Mg dating of CAI rims. Earth Planet. Sci. Lett. 238, 272–283.
- Simon, J. I., DePaolo D. J., and Moynier, F. 2009. Calcium isotopic composition of meteorites, Earth, and Mars. Astrop. vs. J. 702, 707–715.
- Simon, J. I., Cuzzi, J. N., McCain, K., Christoffersen, P., Srinivasan, P., Fisher, K., Tait, A.W., Olson, J. N., and Scargle, J. 2018. Particle size distributions in chondritic meteorites: evidence for pre-planetesimal histories. Earth Planet. Sci. Lett. 494, 69-82.
- Skulan, J. DePaolo, D. J., and Owens, T. L. 1997. Biological control of calcium isotopic abundances in the global calcium cycle. Geochim. Cosmochim. Acta 61, 2505-2510.
- Spicuzza, M. J., Day, J. M. D., Taylor, L. A., and Valley, J. W. 2007. Oxygen isotope constraints on the origin and differentiation of the Moon. Earth Planet. Sci. Lett. 253, 254-265.
- Srinivasan, G., Ulyanov, A. A., and Goswami, J. N. 1994. ⁴¹Ca in the early Solar System. Astrophys. J. 431, L67–L70.

- Srinivasan, G., Sahijpal, S., Ulyanov, A. A., and Goswami, J. N. 1996. Ion microprobe studies of Efremovka CAIs: II. Potassium isotope composition and ⁴¹Ca in the early Solar System. Geochim. Cosmochim. Acta 60,1823–1835.
- Tang, H. and Dauphas, N. 2014. ⁶⁰Fe-⁶⁰Ni chronology of core formation on Mars. Earth Planet. Sci. Lett. 390, 264–274.
- Taylor, S.R and Mason, B. 1978. Chemical Characteristics of Ca-Al Inclusions in the Allende Meteorite. Lunar Planet. Sci. 9, 1158-1160.
- Teng, F. -Z., Li, W. -Y., Ke, S., Marty, B., Dauphas, N., Huang, S., Wu, F. -Y., and Pourmand, A. 2010. Magnesium isotopic composition of the Earth and chondrites. Geochim. Cosmochim. Acta 74, 4150-4166.
- Thiemens, M. H. and Heidenreich, J. E. 1983. The mass-independent fractionation of oxygen: A novel isotope effect and its possible cosmochemical implication. Sc ence 219, 1073-1075.
- Torrano, Z. A., Brennecka, G. A., Williams, C. D., Romanie lo, S. J., Hines, R. R., and Wadhwa, M. Titanium isotope signatures of calcium-aluminum rich inclusions from CV and CK chondrites: Implications for early Solar System reservoirs and mixing. Geochim. Cosmochim. Acta 263, 13-30.
- Trinquier, A., Elliott, T., Ulfbeck, D., Coath, C., Kro', A. N., and Bizzarro, M. 2009. Origin of nucleosynthetic isotope heterogeneity in the Sol r proplanetary disk. Science 324, 374-376.
- Valdes, M. C., Moreira, M., Foriel, J., and Moynier, F. 2014. The nature of Earth's building blocks as revealed by calcium isotopes. Earth Planet. Sci. Lett. 394, 135-145.
- Valdes, M. C., Debaille, V., Berger J. and Armytage, R. M. G. 2019. The effects of high-temperature fractional crystallization of culcium isotopic composition. Chem. Geol. 509, 77-91.
- Wanajo, S. Janka, H.-T., and Muller, B. 2013. Electron-capture supernovae as origin of ⁴⁸Ca. Astrophys. J. 767, #L26 (6 pp)
- Wang, K., Savage, P. S., and Moynier, F. 2014. The iron isotope composition of enstatite meteorites: Implications for heir origin and the metal/sulfide Fe isotopic fractionation factor. Geochim. Cosmochim. A cua 142, 149-165.
- Wark, D. and Boynton, W. V. 2001. The formation of rims on calcium-aluminum-rich inclusions: Step I-flash heating. Meteorit. Planet. Sci. 36, 1135–1166.
- Warren, P. H. 2011. Stable-isotopic anomalies and the accretionary assemblage of the Earth and Mars: a subordinate role for carbonaceous chondrites. Earth Planet. Sci. Lett. 311, 93-100.
- Wasserburg, G. J., Trippella, O., and Busso, M. 2015. Isotope anomalies in the Fe-group elements in meteorites and connections to nucleosynthesis in AGB Stars. Astrophys. J. 805, 7.
- Wasson, J. T. and Kallemeyn, G. W. 1988. Compositions of chondrites. Philos. Trans. R. Soc. A 325, 535–544.
- Wasson, J. T. and Wetherill, G. W. 1979. Dynamical chemical and isotopic evidence regarding the formation locations of asteroids and meteorites. In: Asteroids (Ed. Gehrels, T.), University of Arizona Press, Tucson, 926-974.

- Weber, D., Zinner, E. K., and Bischoff, A. 1995. Trace element abundances and magnesium, calcium, and titanium isotopic compositions of grossite-containing inclusions from the carbonaceous chondrite Acfer 182. Geochim. Cosmochim. Acta 59, 803–823.
- Weisberg, M. K., McCoy, T. J., and Krot, A. N. 2006. Systematics and evaluation of meteorite classification. In: Meteorites and the Early Solar System II (Eds. Lauretta, D. S. and McSween, H. Y. Jr.), University of Arizona Press, Tucson, 19-52.
- Wiechert, U., Halliday, A. N., Lee, D. -C., Snyder, G. A., and Rumble, D. 2001. Oxygen isotopes and the Moon-forming giant impact. Science 294, 345-348.
- Wimpenny, J. B., Yin, Q. Z., Zipfel, J., MacPherson, G., Ebel, D. S., and Heck, P. R. 2014. Renewed search for FUN based on Al-Mg systematics in CAIs with LA-MC-ICP-MS. Lunar Planet. Sci. 45, #2235.
- Wood, J. A. 2005. The chondrite types and their origins. In: A.N. Krot, E.R.D. Scott, and B. Reipurth (eds.), Chondrites and the Protoplanetary Disk, ASP conference Series, 953–971.
- Worsham, E. A., Bermingham, K. R., and Walker, R. J. 2017. Characterizing cosmochemical materials with genetic affinities to the Earth: Genetic at d Cyronological diversity within the IAB iron meteorite complex. Earth Planet. Sci. Lett. 467, 157-166.
- Yamada, M., Tachibana, S., Nagahara, H., and Ozava, K. 2006. Anisotropy of Mg isotopic fractionation during evaporation and Mg self-diffusion of forsterite in vacuum. Planet. Space Sci. 54, 1096–1106.
- Yin, Q.-Z., Yamashita, K., Yamakawa, A., Tanaka, R., Jacobsen, B., Ebel, D. S., Hutcheon, I. D., and Nakamura, E. 2009. 53 Mn- 53 Cr systematics of Allende chondrules and epsilon 54 Cr- Δ^{17} O correlation in bulk carbonaceous chor dr. S. Lunar Planet. Sci. 40, #2006.
- Yokoyama, T., Misawa, K., Okano, C., Shih, C.-Y., Nyquist, L. E., Simon, J. I., Tappa, M. J., and Yoneda, S. 2017. Extreme rarly Solar System chemical fractionation recorded by alkali-rich clasts contained in ordinary chemical breccias. Earth Planet. Sci. Lett. 458, 233–240.
- Yoneda, S. and Grossmar, L. 1795. Condensation of CaO-MgO-Al₂O₃-SiO₂ liquids from cosmic gases. Geochim. Cosm. co. im Acta 59, 3413-3444.
- Young, E. D., Nagahara J., Mysen, B. O., and Audet, D. M. 1998. Non-rayleigh oxygen isotope fractionation by mineral evaporation: Theory and experiments in the system SiO₂. Geochim. Cosmochim. Acta 62, 3109–3116.
- Young, E. D., Galy, A., and Nagahara, H. 2002. Kinetic and equilibrium mass-dependent isotope fractionation laws in nature and their geochemical and cosmochemical significance. Geochim. Cosmochim. Acta 66, 1095-1104.
- Young, E. D., Kohl, I. E., Warren, P. H., Rubie, D. C., Jacobson, S. A., and Morbidelli, A. 2016. Oxygen isotopic evidence for vigorous mixing during the Moon-forming giant impact. Science 351, 493-496.
- Zhang, J., Dauphas, N., Davis, A. M., Leya, I., and Fedkin, A. 2012. The proto-Earth as a significant source of lunar material. Nat. Geosci. 5, 251–255.

Zhang, J., Huang, S., Davis, A. M., Dauphas, N., Hashimoto, A., and Jacobsen, S. B. 2014. Calcium and titanium isotopic fractionations during evaporation. Geochim. Cosmochim. Acta 140, 365–380.

Zinner, E. 2014. PreSolar grains. In: Meteorites and Cosmochemical Processes (Ed. Davis, A. M.), Vol. 1 Treatise on Geochemistry, 2nd Ed. (Exec. Eds. Holland, H. D. and Turekian, K. K.), Elsevier, Oxford, 181–213.

Zinner, E., Fahey, A. J., McKeegan, K. D., Goswami, J. N., and Ireland, T. R. 1986. Large ⁴⁸Ca anomalies are associated with ⁵⁰Ti anomalies in Murchison and Murray hibonites. Astrophys. J. 311, L103–L107.

Zinner, E., Tang, M., and Anders, E. 1987. Large isotopic anomalies of Si, C, N, and noble gases in interstellar silicon carbide from the Murray meteorite. Nature 33: 730-732.

Zolensky, M. E. and McSween, H. Y. 1988. Aqueous alteration. In: Kerridge, J. F. and Matthews, M. S (eds.), Meteorites and the Early Solar System, University of Arizona Press, 114–143.

Table 1. Stable Ca isotopes, their natural abundances, and nucleosynthetic pathways of production.

Isotope	Natural abundance	Nucleosynthesis	
⁴⁰ Ca	96.941	O and Si-burning	
⁴¹ Ca [*]	-	Neutron capture on ⁴⁰ Ca	
⁴² Ca	0.647	O and Si-burning	
⁴³ Ca	0.135	O and Si-burning	
⁴⁴ Ca	2.036	Decay product of ⁴⁴ Ti [#] , produced during O and Si-burning	
⁴⁶ Ca	7.0(4	s-process	
⁴⁸ Ca [‡]	(.187	Neutron-rich processes: Type Ia or e ⁻ capture SN of AGB	

 $^{^{*41}}$ Ca ($t_{1/2} = 103 \text{ ka}$)

Table 2. Typical REE patterns seen in silicate CAIs (from Mason and Taylor, 1982)

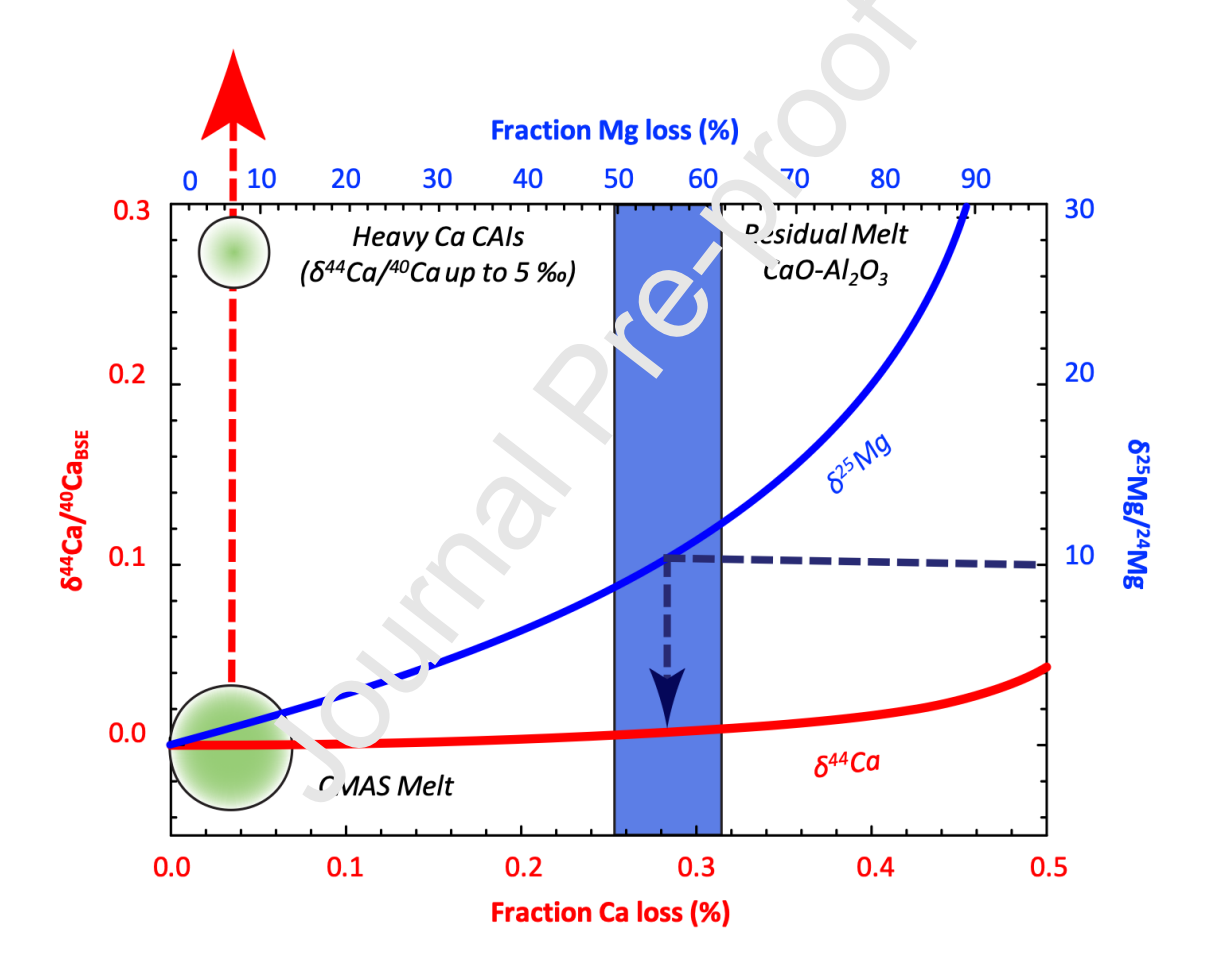
Group	REE fractionation pattern	Abundance (rel. to CI chondrite)
I	Relatively unfractionated (excepting a small positive Eu anomaly)	~10-15

 $^{^{#44}}$ Ti ($t_{1/2} = 60 a$)

 $^{^{\}downarrow}$ ⁴⁸Ca is radioactive ($t_{1/2}$ = 4.3 x 10^{19} a); however, its long half-live permits it to be considered a stable isotope

II	Highly fractionated, with depletion of the heavy lanthanides (Gd-Er) and Eu, and positive Tm and Yb anomalies	< 1 to 20
III	Unfractionated (excepting negative Eu and Yb anomalies)	~20
IV	Relatively unfractionated	~2-4
V	Relatively unfractionated	~10-20
VI	Relatively unfractionated (excepting positive Eu and Yb anomalies)	~10-20

Figure 1.



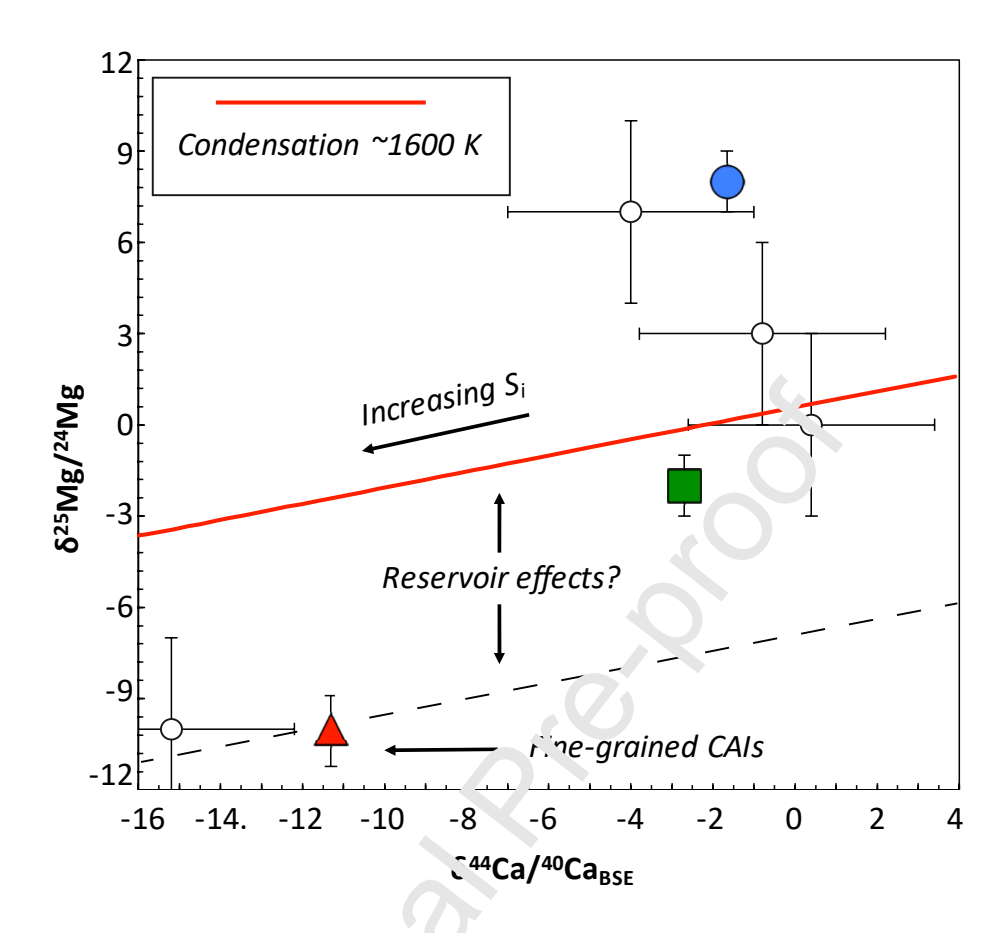


Figure 2.

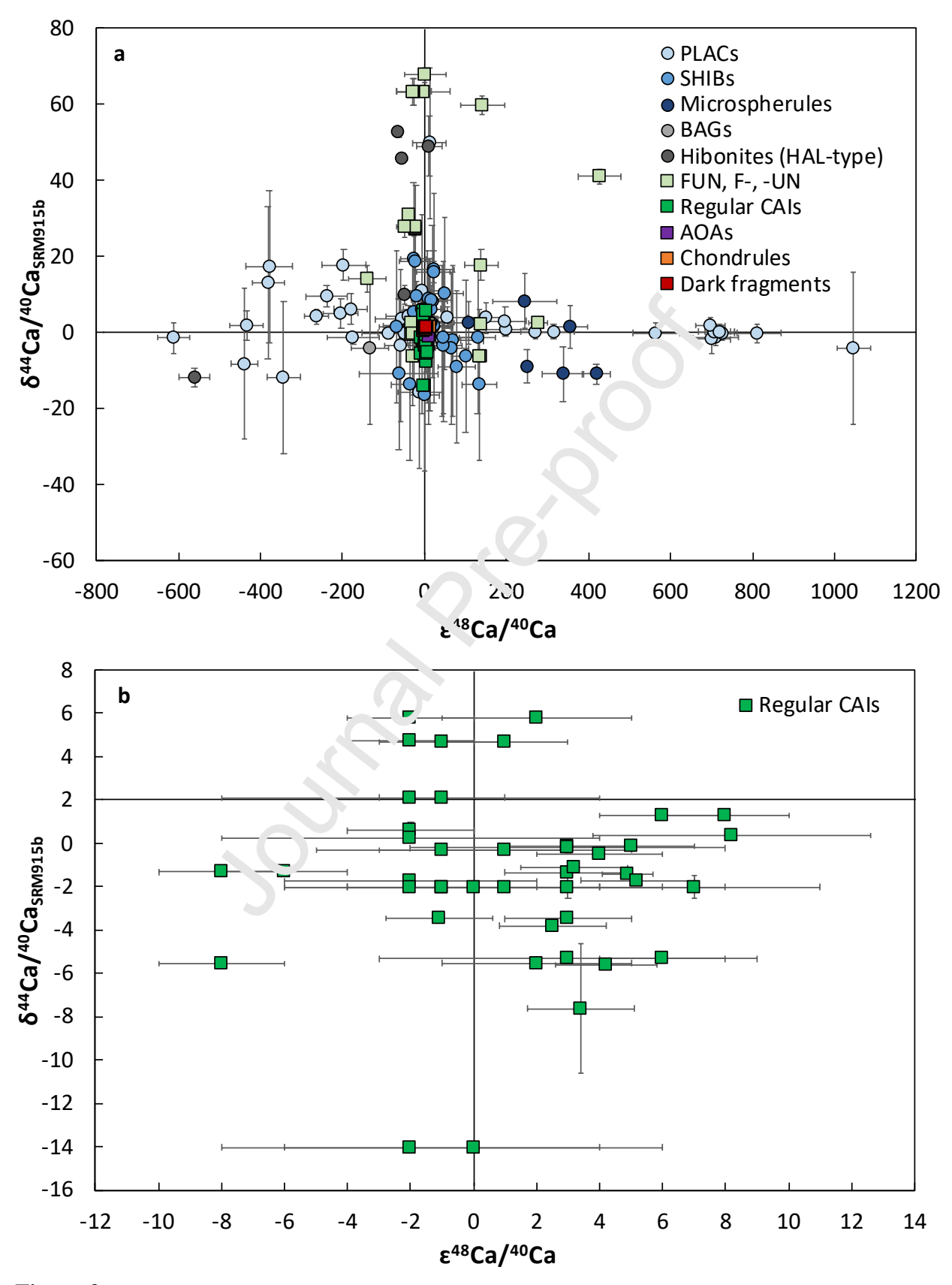


Figure 3.

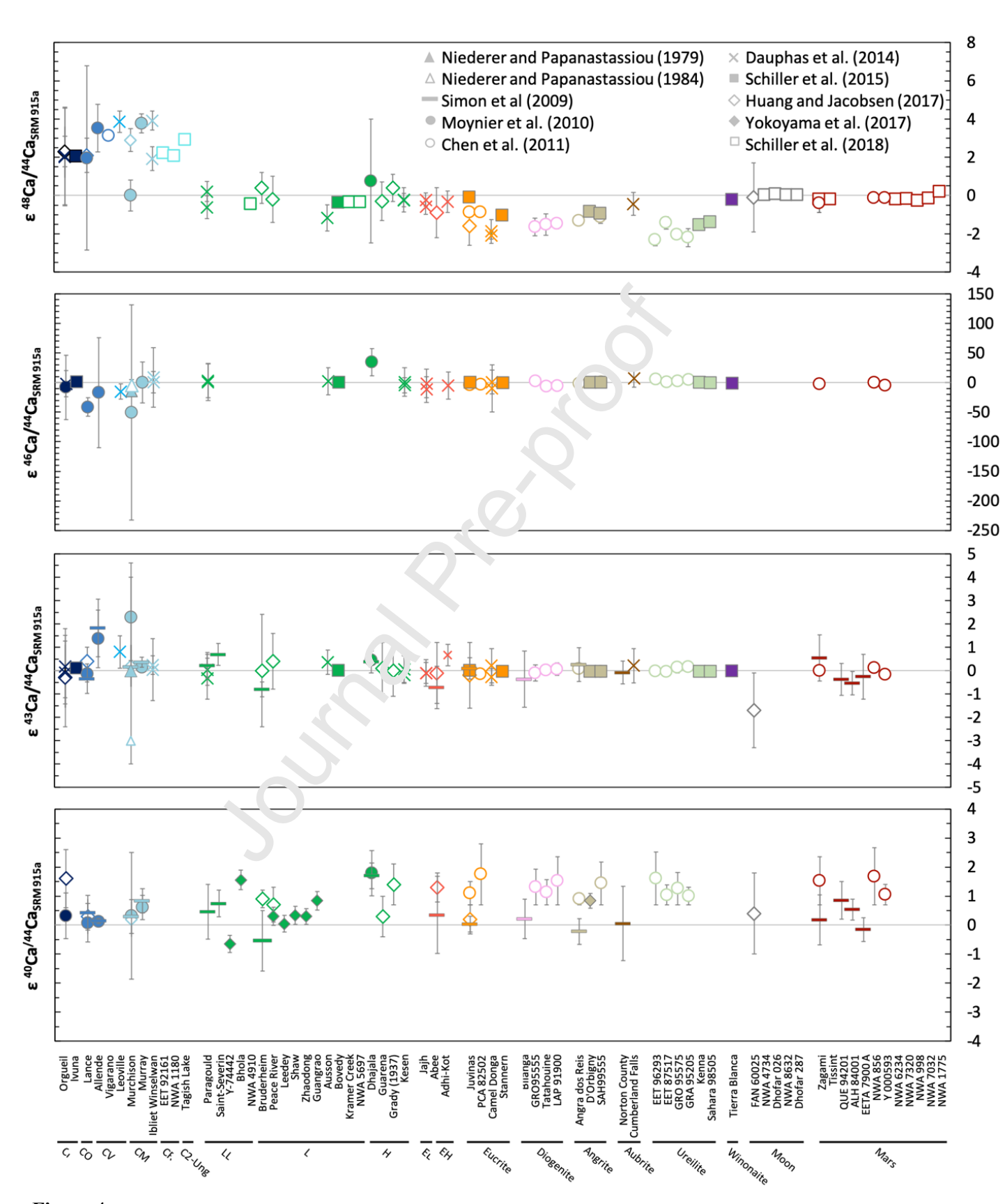


Figure 4.

Figure 5.

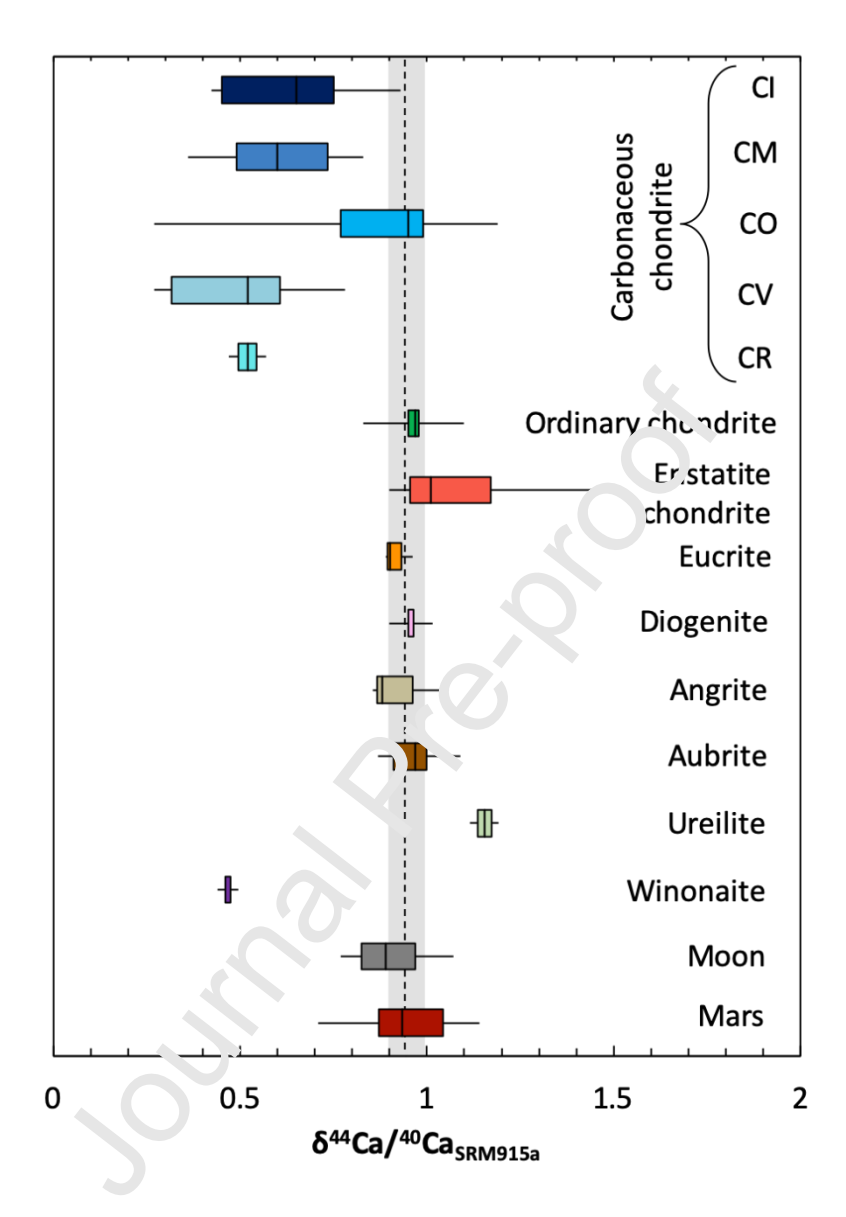


Figure captions

- Figure 1. Modeled Rayleigh-like isotope fractionation due to evaporation of CAI-like precursors; Ca-red and Mg-blue curves are calculated by Simon and DePaolo (2010). This work shows how CAIs with high δ^{44} Ca/ 40 Ca compositions record at least two and likely three distinct nebular events, the first involved extensive high temperature evaporation leading to Ca isotope fractionation, the second included significant Mg (and Si) addition, and the third involved additional evaporation leading to fractionated high $\delta^{25} Mg^{/24} Mg$ compositions. Complete (>99%) evaporative loss of Mg is implied by CAIs with high δ^{44} Ca^{/40}Ca compositions (off-scale) (Niederer and Papanastassiou, 1984) (i.e., heavier than all values of Ca-curve). Based on the fraction of Ca loss implied by the typical Mg isotopes of CAIs (i.e. upper range shown by blue column), minimal fractionation should exist. The models tack changes in residual melt composition during evaporative loss of MgO, SiO₂, Al₂O₃, and CaO and match experiments of Richter et al. (2002). Once CaO and Al₂O₃ dominate the regidue (≥80% Mg loss) evaporation rates of CMAS melts are less well understood and isotonic fractionation models that assume a constant evaporation coefficient for calcium (e.g., Simo, and DePaolo, 2010; Shahar and Young, 2007; Richter et al., 2002; Young et al., 1998) match experiments less well. Calcium dominated evaporation experiments of Zhang et al. (2014) rdi ate ~4x greater Ca isotope fractionation, which is still broadly consistent with the models shown, but indicate the need for refined models that more accurately account for changing ave poration rates and the chemical species pertinent to evaporation of materials that are largely mach of CaO and Al₂O₃. Simon and DePaolo (2010) define δ^{44} Ca/ 40 Ca = 0 as the BSE composition, which has a value of +0.95 relative to the Ca standard SRM915a (see Section 2.1).
- **Figure 2.** δ^{44} Ca/ 40 Ca and δ^{25} M. $7/^{24}$ Mg as a function of oversaturation (S_i) calculated from the condensation model of Simon s^4 al. (2017). Double-spike Ca TIMS data (Simon et al., 2017; Huang et al. 2012) coupled with MC-ICPMS Mg data (Bullock et al., 2013; Jordan et al. 2013) for several CAIs (type B, blue circle; type B forsterite bearing, green square; and type A fine-grained, red triangle) and early data of Niederer and Papanastassiou (1984) (open circles) are shown. These authors define δ^{44} Ca/ 40 Ca = 0 as the BSE composition, which has a value of +0.95 relative to the Ca standard SRM915a (see **Section 2.1**).
- **Figure 3.** Non-mass-dependent $(\delta^{44}\text{Ca})^{40}\text{Ca})$ vs. mass-dependent $(\epsilon^{48}\text{Ca})^{44}\text{Ca})$ isotopic compositions obtained from the same meteorite component. Error bars are those reported in the original publications. Mass-dependent data reported relative to SRM915a. The area around the origin in (a) is shown in (b) displaying regular CAIs only.
- **Figure 4.** Non-mass-dependent ε^{40} Ca^{/44}Ca, ε^{43} Ca^{/44}Ca, ε^{46} Ca^{/44}Ca, and ε^{48} Ca^{/44}Ca isotopic compositions of chondrites, achondrites, lunar samples, and Martian samples. Error bars are those reported in the original publications. Error bars smaller than data points are not shown.

Figure 5. Mass-dependent δ^{44} Ca/ 40 Ca compositions of chondrites, achondrites, lunar samples, and Martian samples. Data have all been renormalized to Ca standard SRM915a. Boxes represent the spread of data about the median and the "error bars" indicate outliers. Data are from Niederer and Papanastassiou (1979, 1984), Simon and DePaolo (2010), Valdes et al. (2014), Magna et al (2015), Schiller et al. (2015), Amsellem et al (2017), Huang and Jacobsen (2017), Simon et al. (2017), Bermingham et al. (2018), and Schiller et al. (2018). The dotted line and grey band represent the BSE estimate of Kang et al. (2017), 0.95 ± 0.05 .